

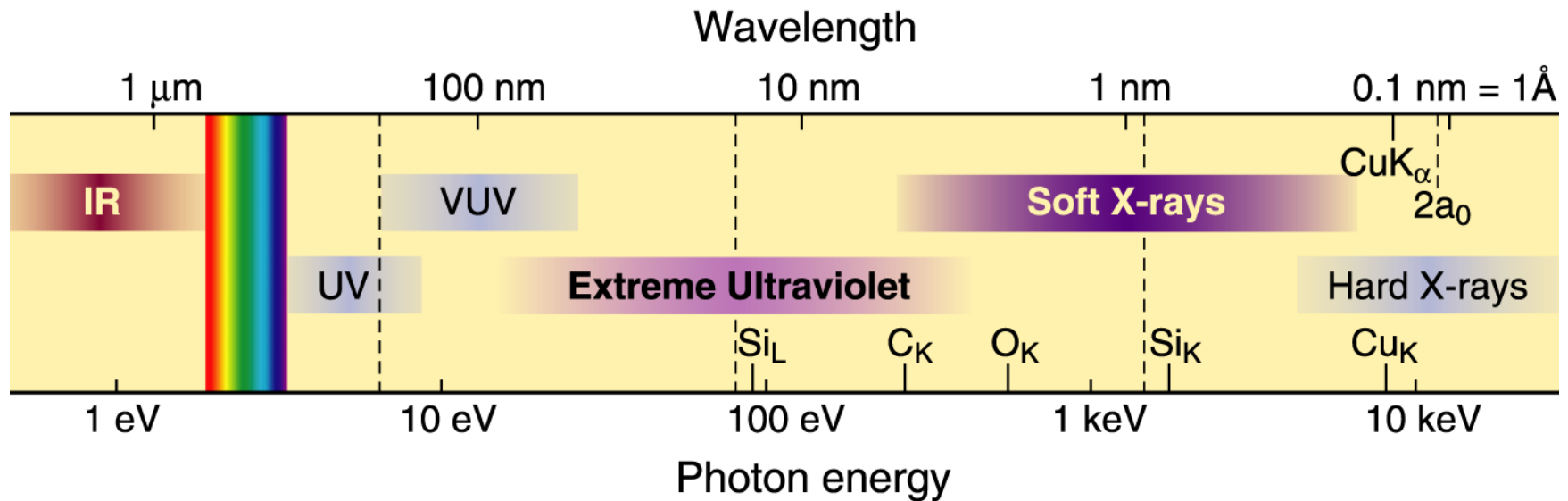


# Hard and Soft X-Ray Microscopy

David Attwood  
University of California, Berkeley

Cheiron School  
September 27, 2014  
SPring-8

# The short wavelength region of the electromagnetic spectrum

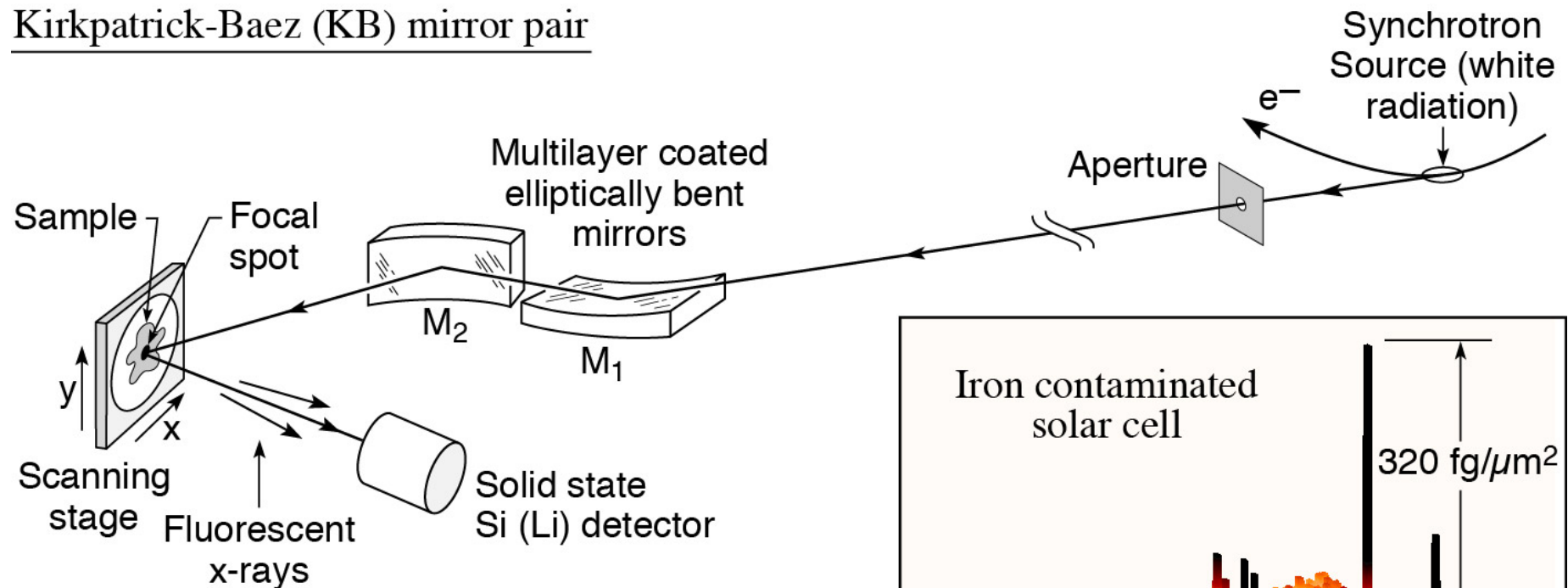


- See smaller features
- Write smaller patterns
- Elemental and chemical sensitivity

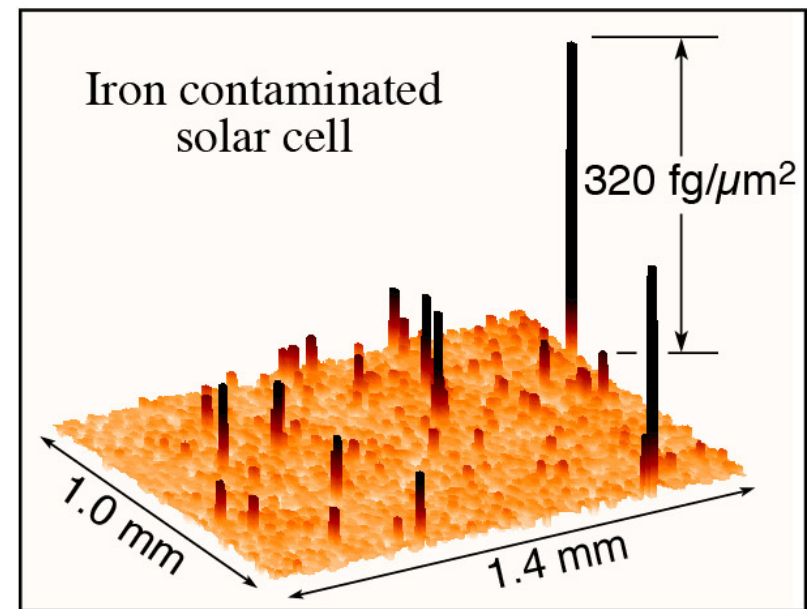
$$\hbar\omega \cdot \lambda = hc = 1239.842 \text{ eV nm}$$

$$n = 1 - \delta + i\beta \quad \delta, \beta \ll 1$$

## Kirkpatrick-Baez (KB) mirror pair



- Crossed cylinders at glancing incidence
- Photon in / photon out, low noise background
- Femtogram and part per billion (ppb) sensitivity
- Micron focus (1988), now  $\sim 25$  nm (Yamauchi, Mimura and colleagues, Osaka U./SPring-8)



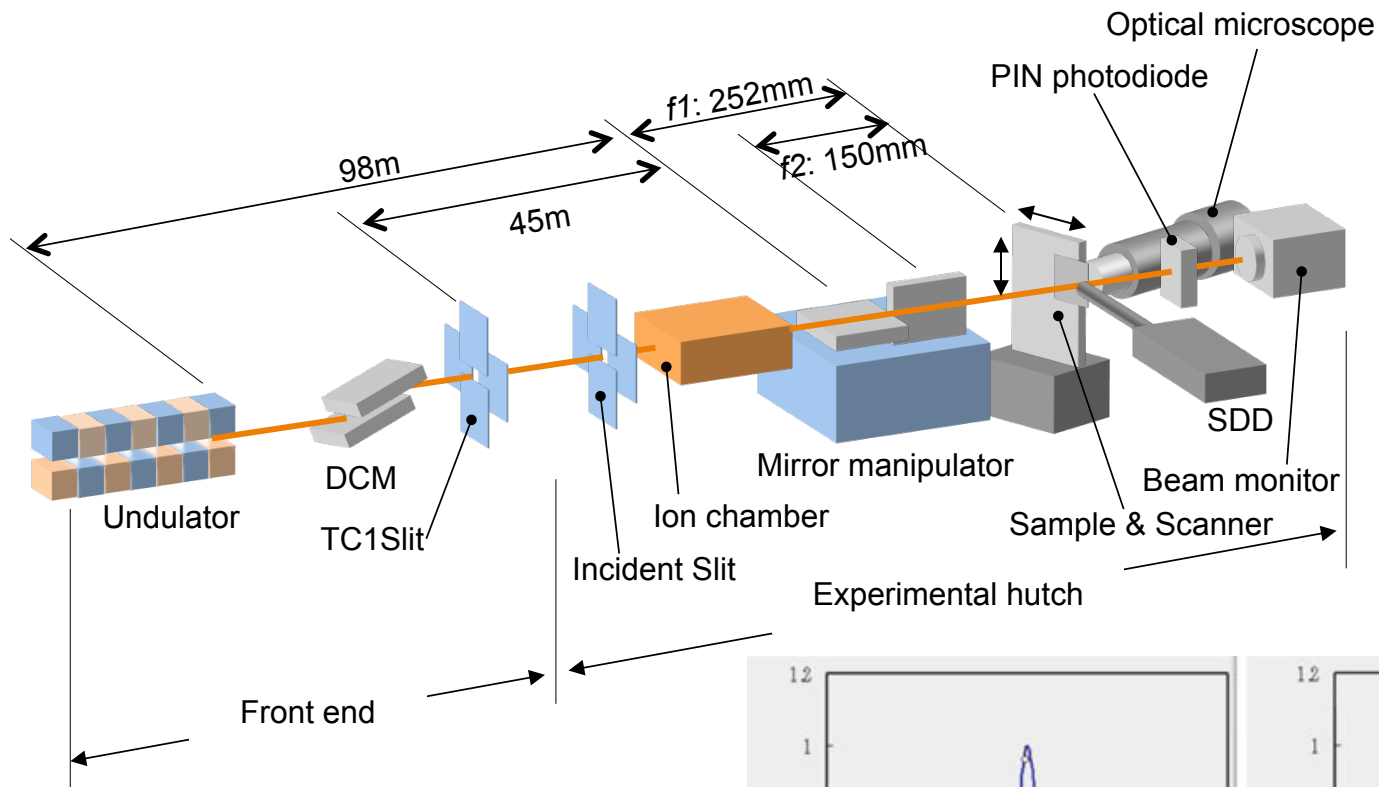
(Courtesy of A. Thompson and J. Underwood, LBNL; and R. Holm, Miles Lab)

FluoresMicroprobe\_August2014.ai

J.H. Underwood and A.C. Thompson, NIM A266, 296 & 318 (1988).

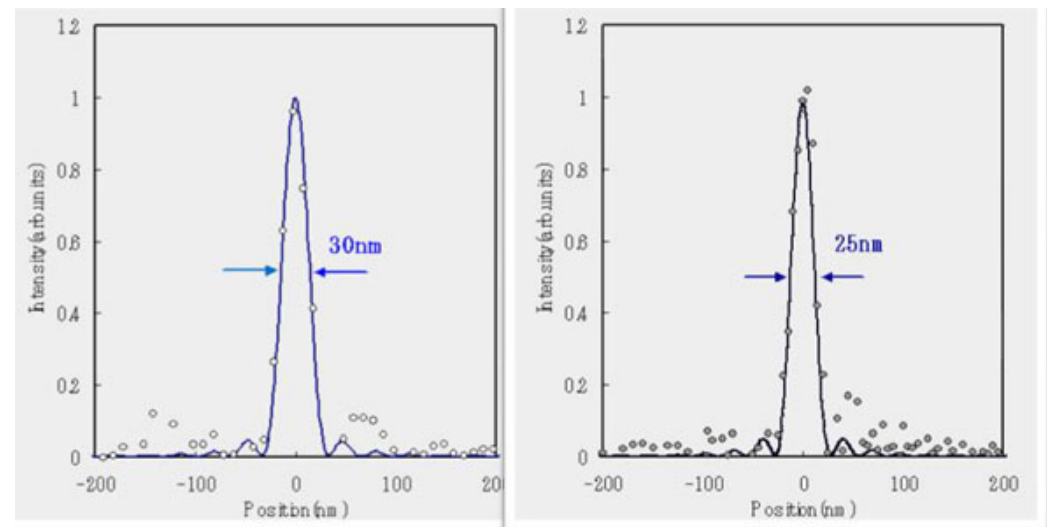


# X-ray microprobe at SPring-8



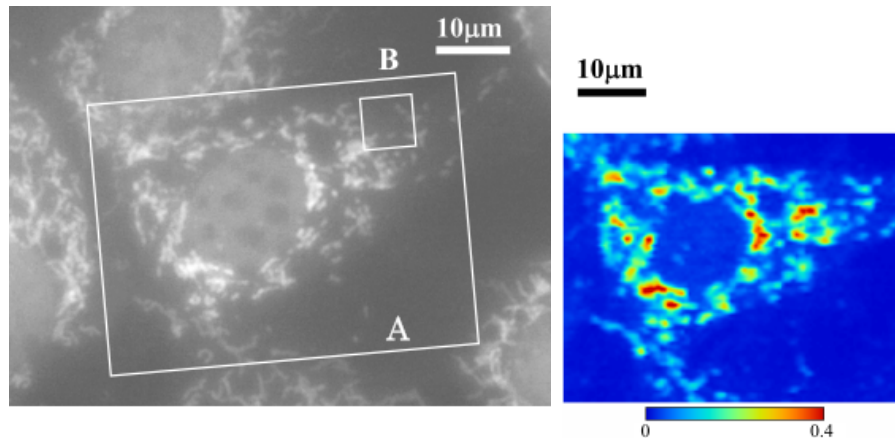
S. Matsuyama et al.,  
Rev. Sci. Instrum.  
77, 103102 (2006)

Courtesy of K. Yamauchi and  
H. Mimura, Osaka University.

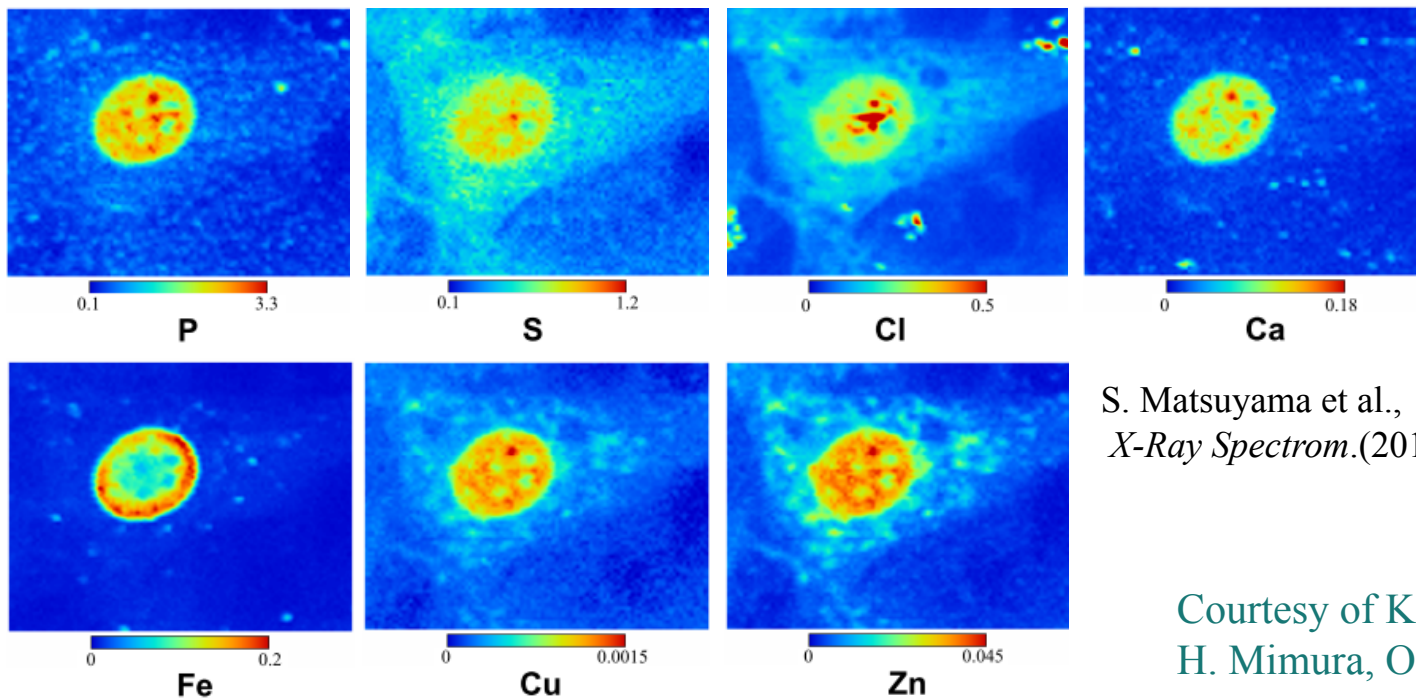




# Sub-cellular elemental analysis using the hard x-ray fluorescence microprobe at SPring-8



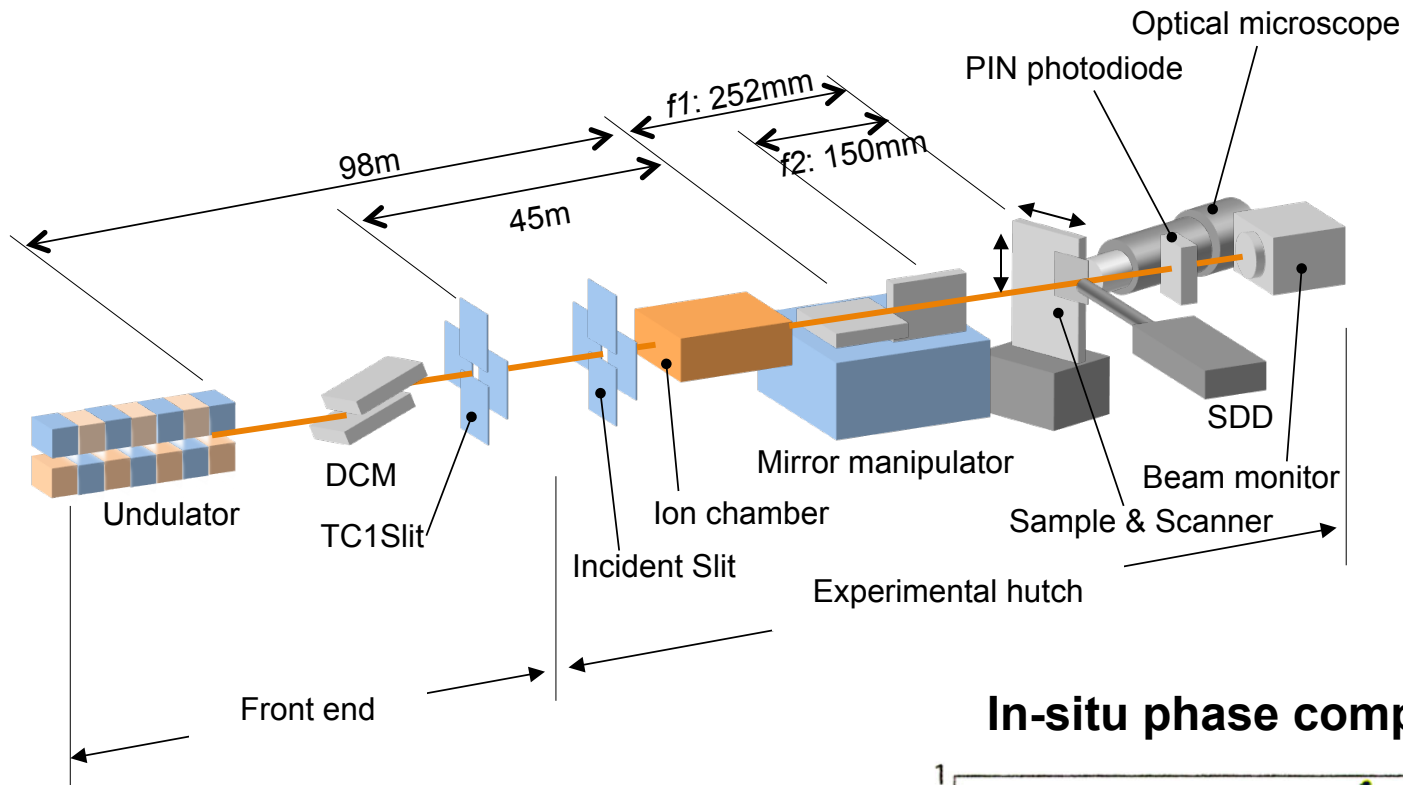
Fluorescent microscope image



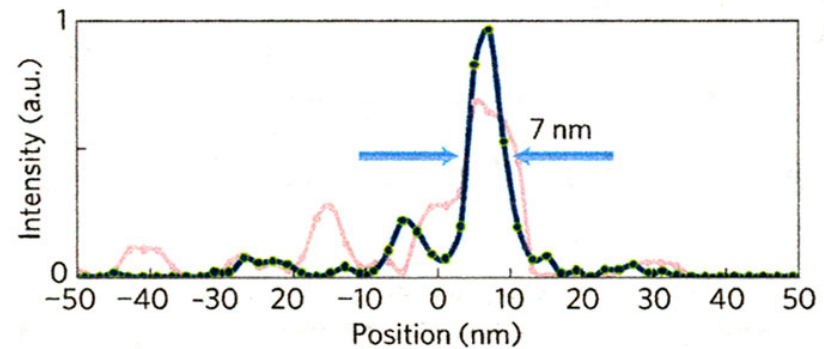
S. Matsuyama et al.,  
*X-Ray Spectrom.*(2010).

Courtesy of K. Yamauchi and  
H. Mimura, Osaka University.

# X-ray microprobe at SPring-8



## In-situ phase compensation

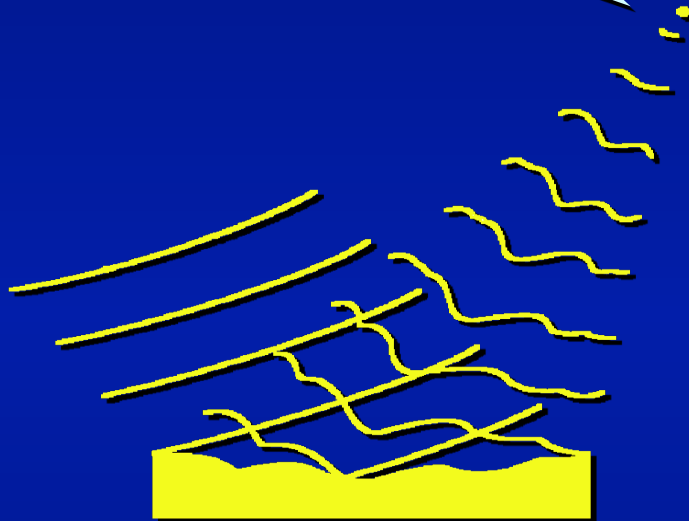
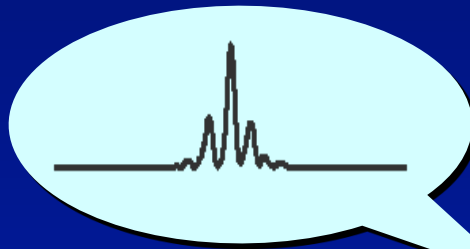


Courtesy of K. Yamauchi and  
H. Mimura, Osaka University.

H. Mimura et al., *Nature Physics*, **6**, 122 (2009)

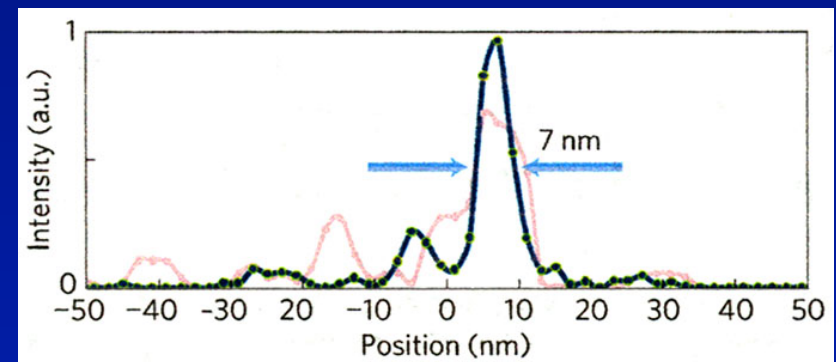
# Breaking the 10 nm barrier in hard x-ray focusing

7

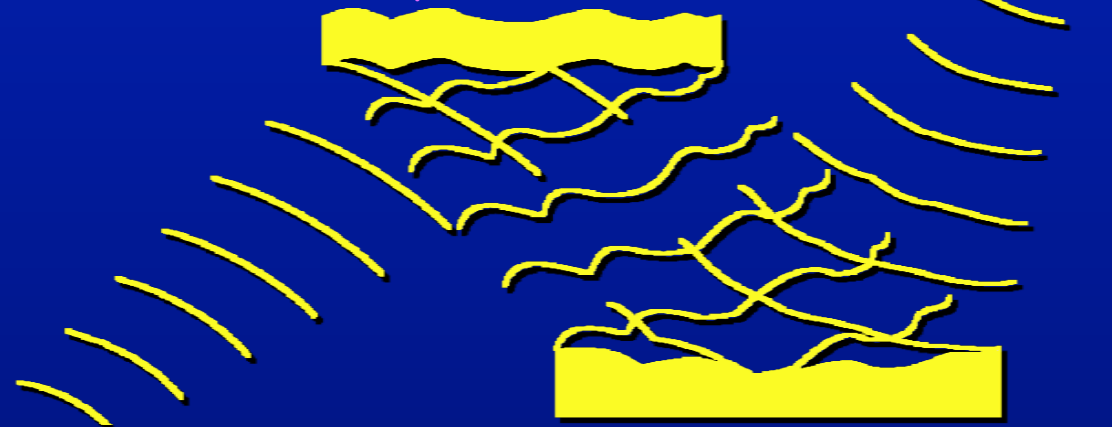


Focusing mirror with phase error

*In-situ phase compensation*



*Piezo-electric phase compensator*

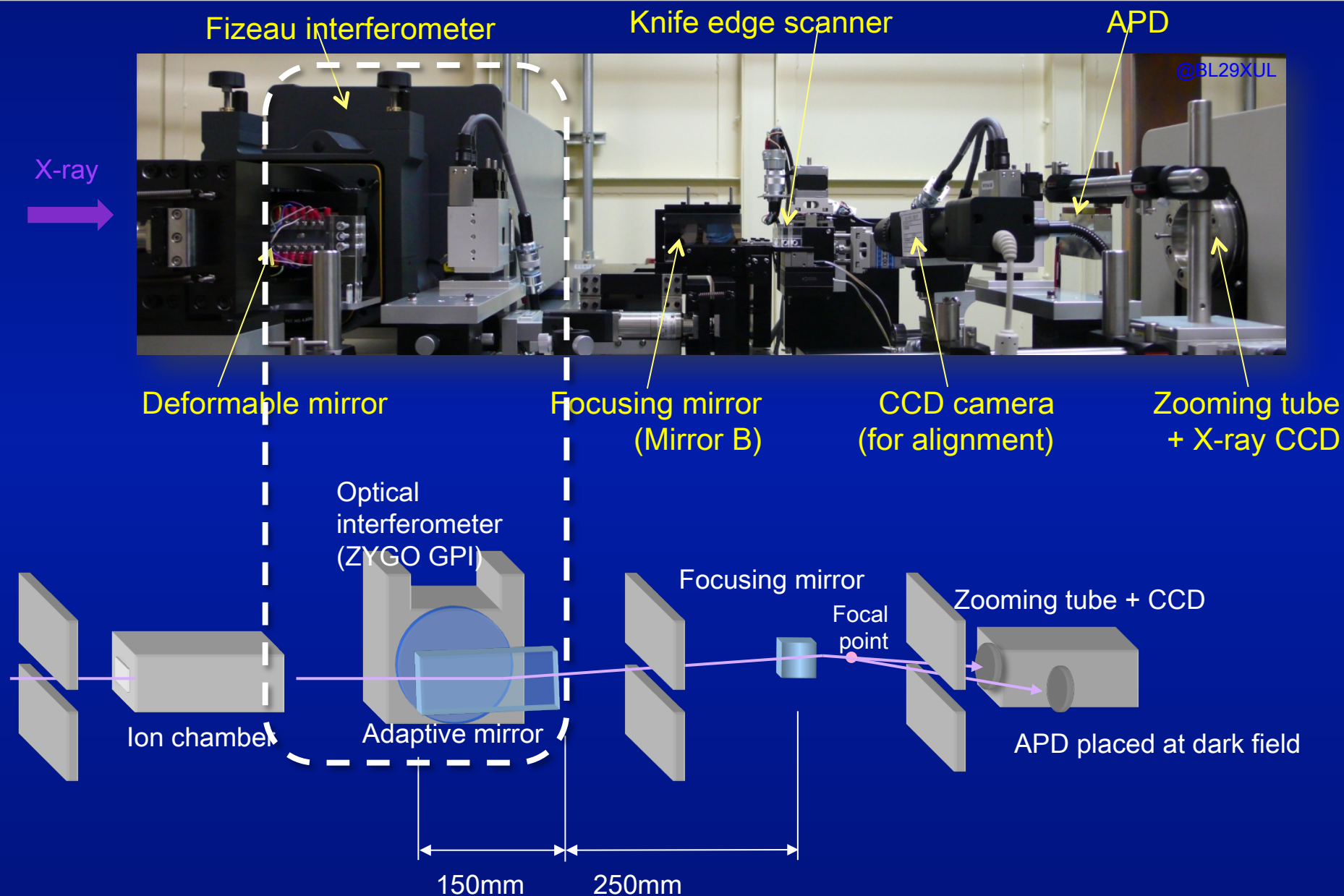


Focusing mirror with phase error

H. Mimura et al., *Nature Physics*, **6**, 122 (2009)

# Optical configuration for active phase compensation

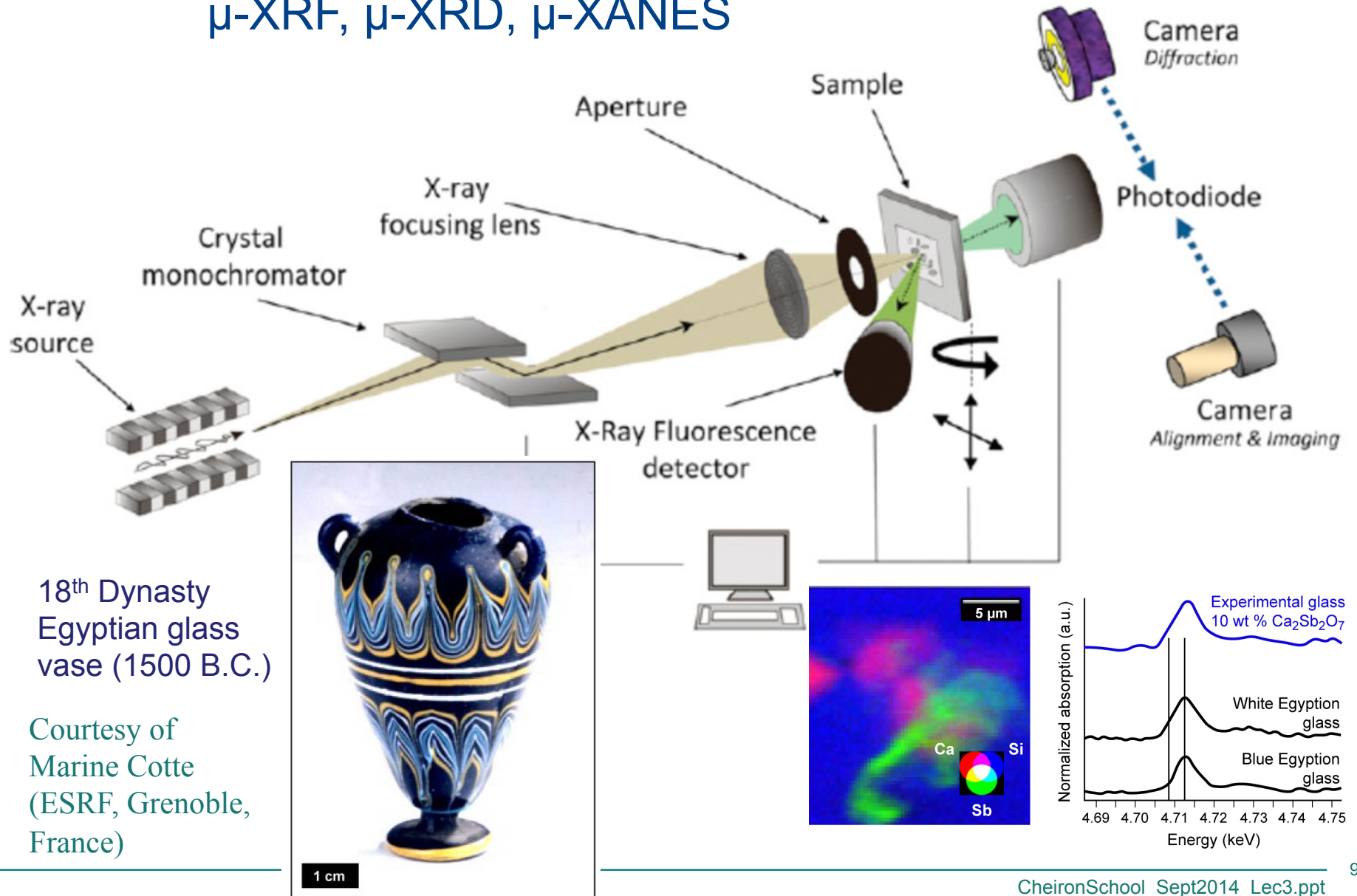
8



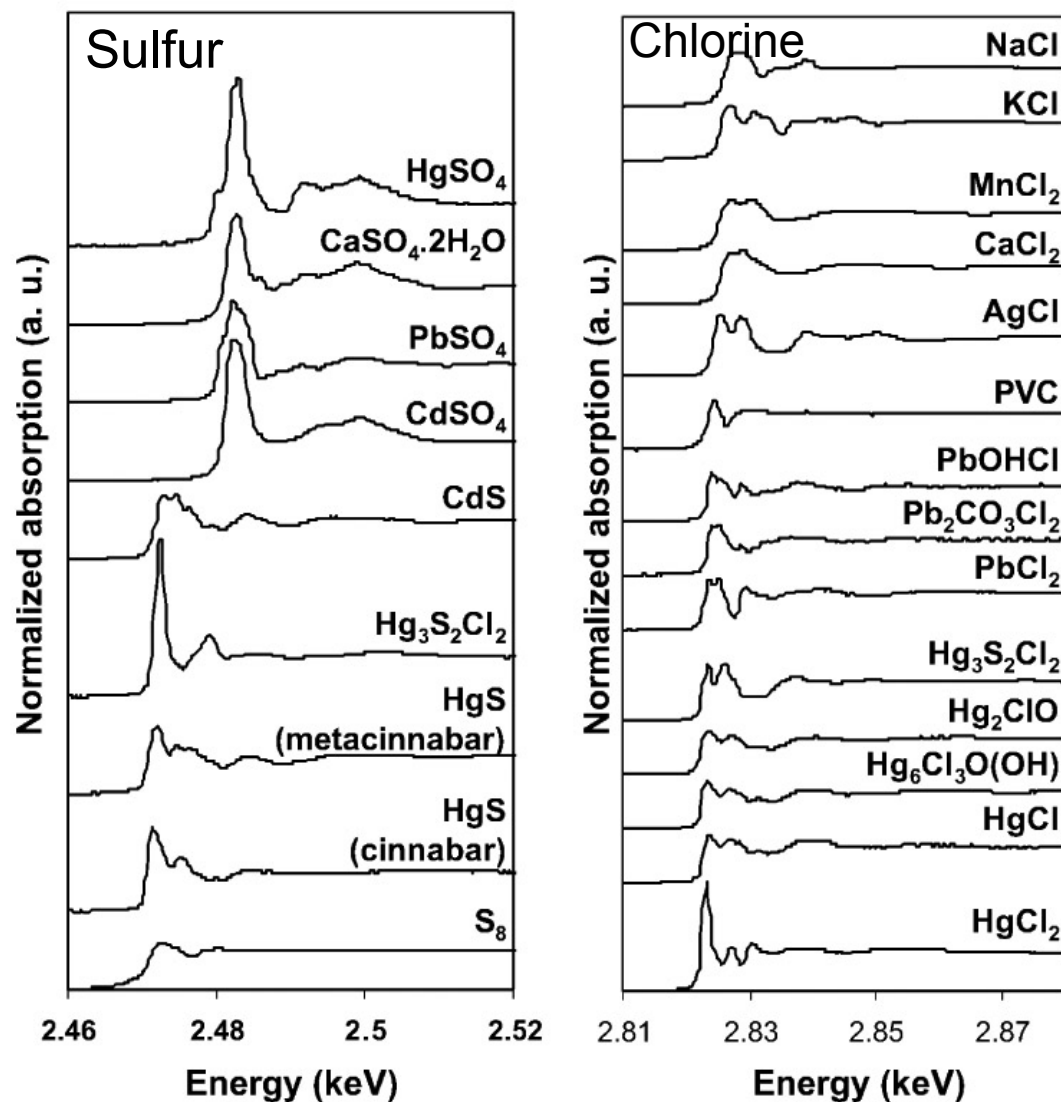


# Synchrotron-based art conservation at ESRF

$\mu$ -XRF,  $\mu$ -XRD,  $\mu$ -XANES



# Examples of $\mu$ -XANES K-edge spectra occurring in art materials

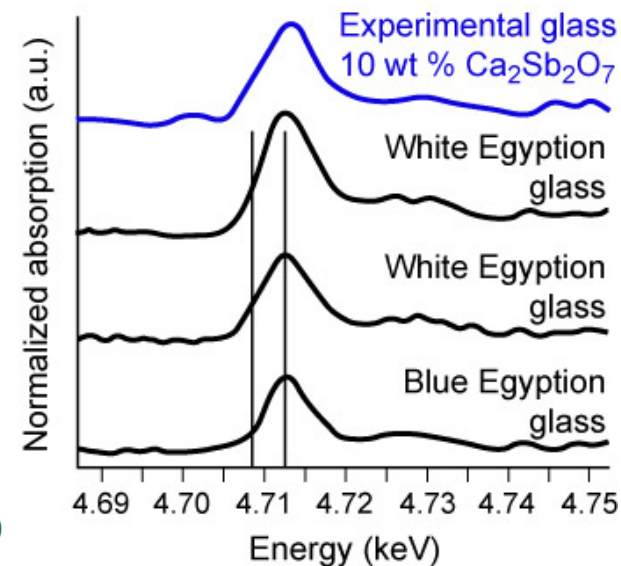
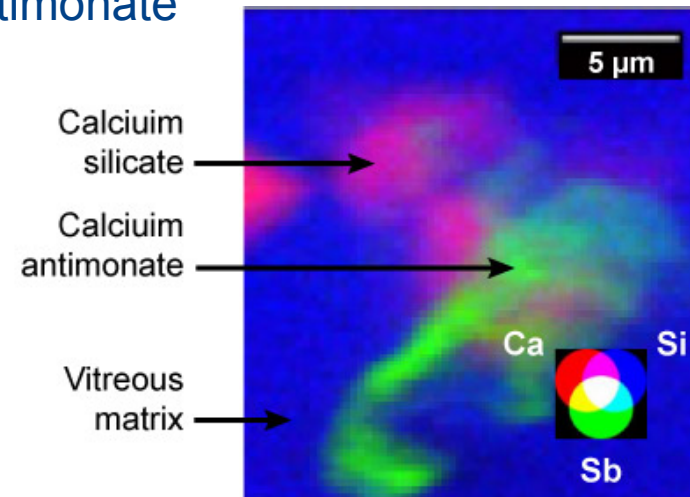


Courtesy of Marine Cotte (ESRF, Grenoble, France)

# 18<sup>th</sup> Dynasty Egyptian glass vase studied for an understanding of color and opaqueness in antiquity



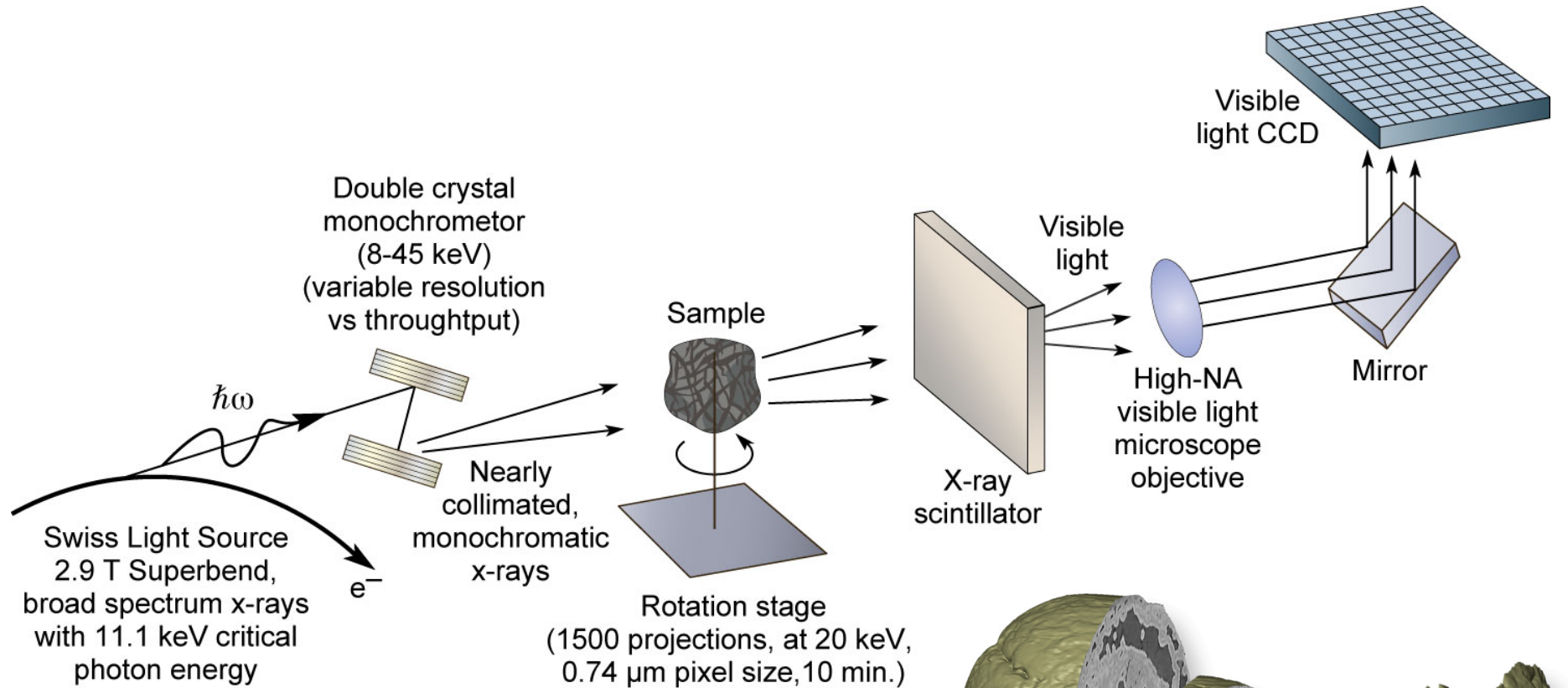
1<sup>st</sup> production of glass objects Egypt (1500 B.C.),  
opaque, colored, nanoscale calcium antimonate



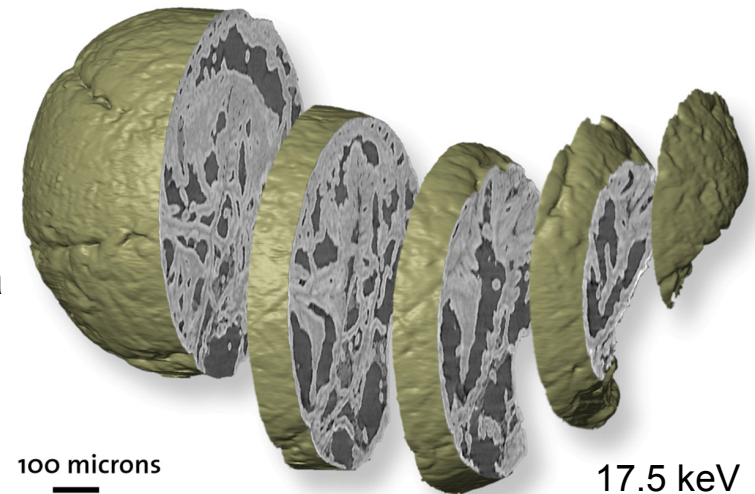
Courtesy of Marine Cotte (ESRF, Grenoble, France)



# Synchrotron radiation x-ray tomographic microscopy (SRXTM)



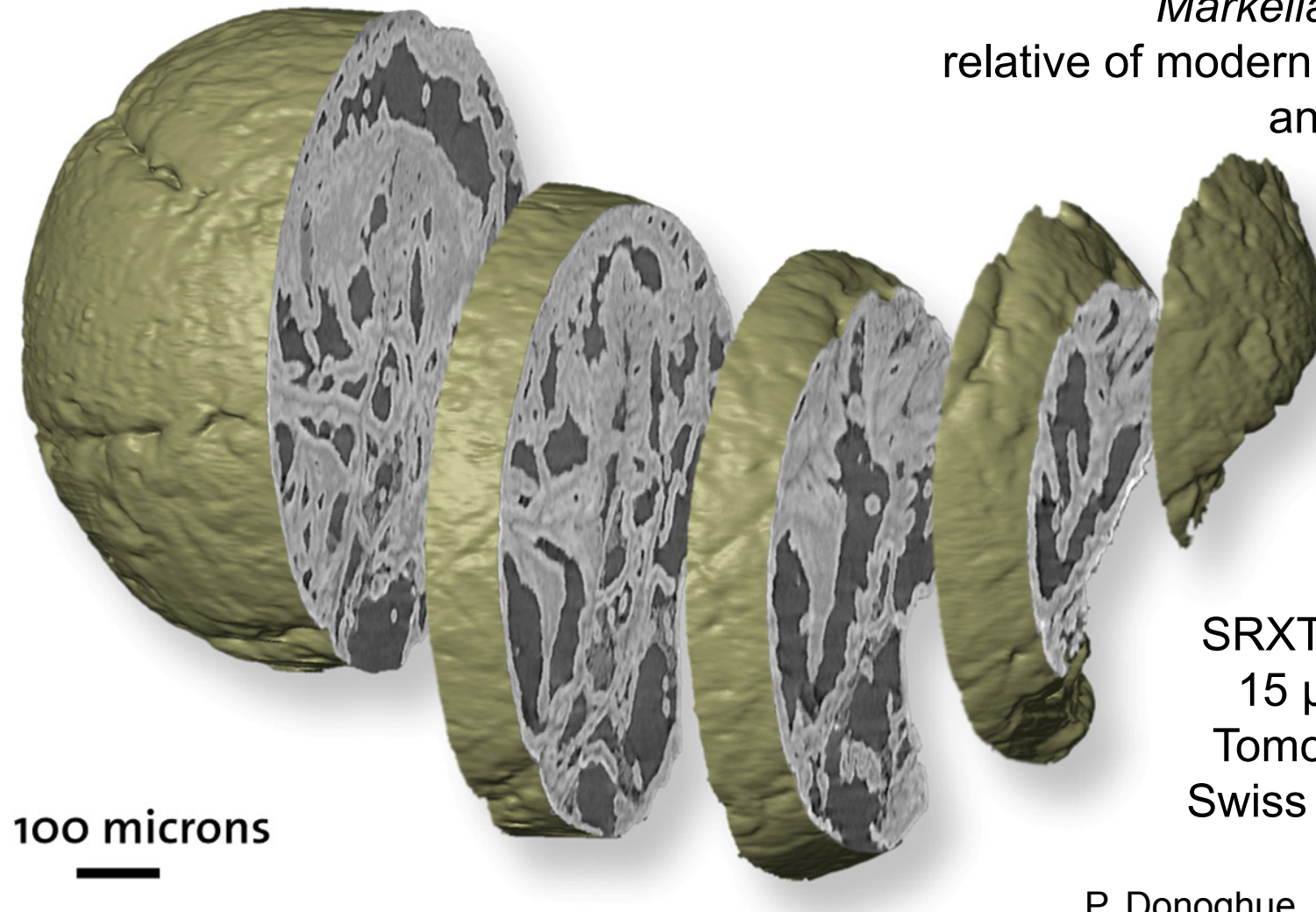
Tomographic reconstruction of a 500 million year old fossilized embryo from Southern China



P. Donoghue, S. Bengtson, M. Stampanoni et al., *Nature* 442, (2006)

# Tomographic reconstruction of a 500 million year old fossilized embryo from Southern China

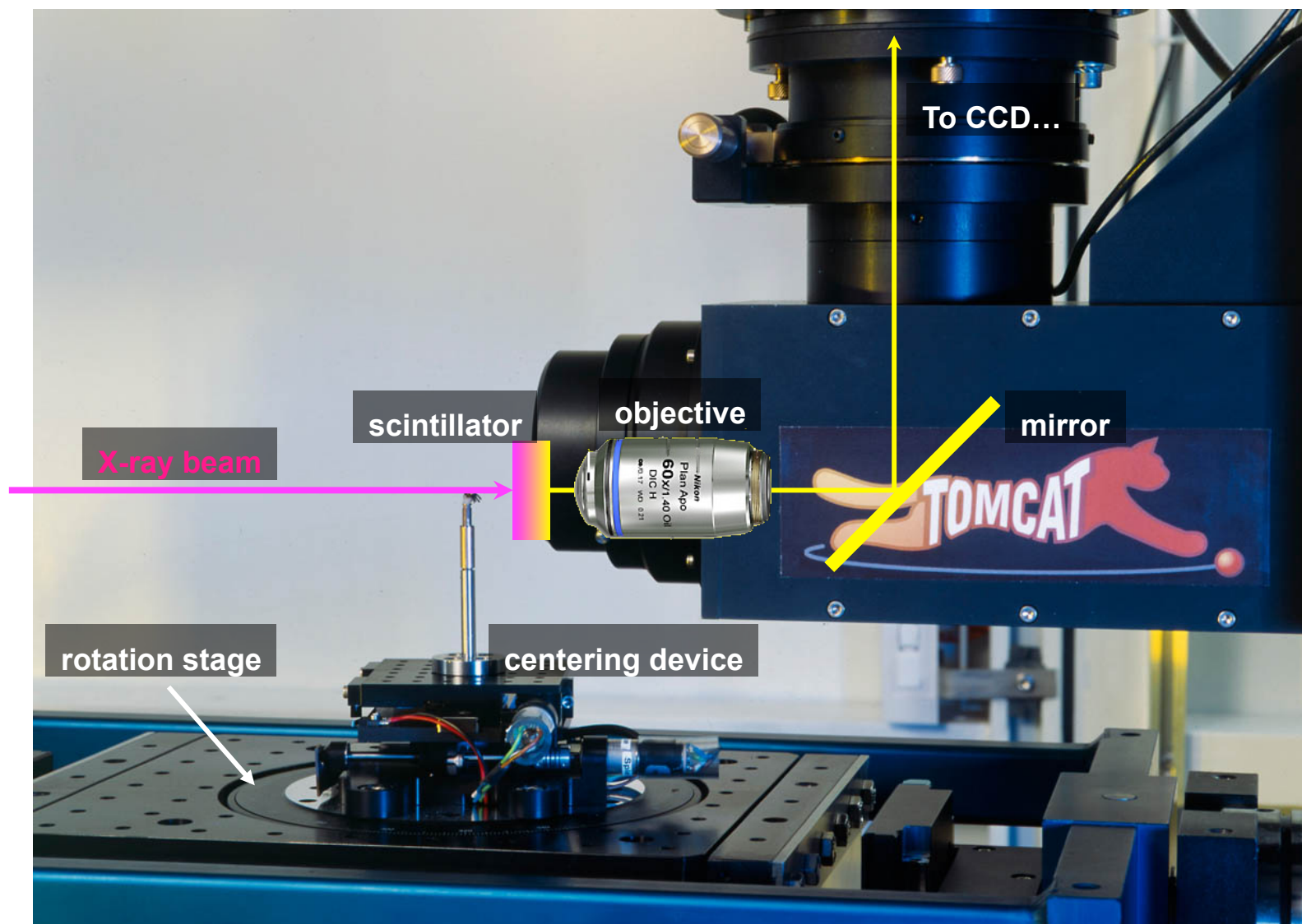
*Markelia hunanensis*  
relative of modern roundworms  
and arthropods



SRXTM, 17.5 keV,  
15  $\mu\text{m}$  resolution  
Tomcat Beamline,  
Swiss Light Source

P. Donoghue, S. Bengtson, M.  
Stampanoni et al., *Nature* 442, (2006)

# TOMCAT Microscope





## Hard x-ray 3D x-ray tomography: microvascular architecture of a mouse brain

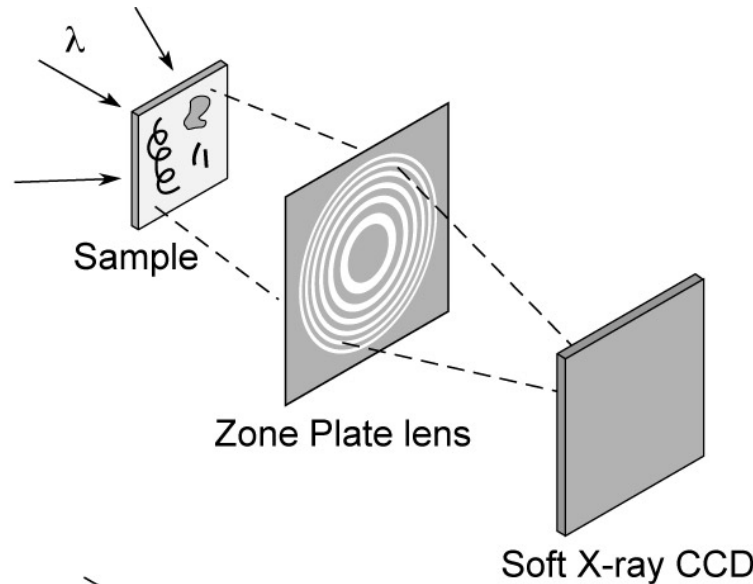


SRXTM, 25 keV,  
15  $\mu\text{m}$  resolution  
Tomcat Beamline,  
Swiss Light Source

M. Stampanoni,  
T. Krucker et al.,  
*Adv. Neur. Res.* (2008)

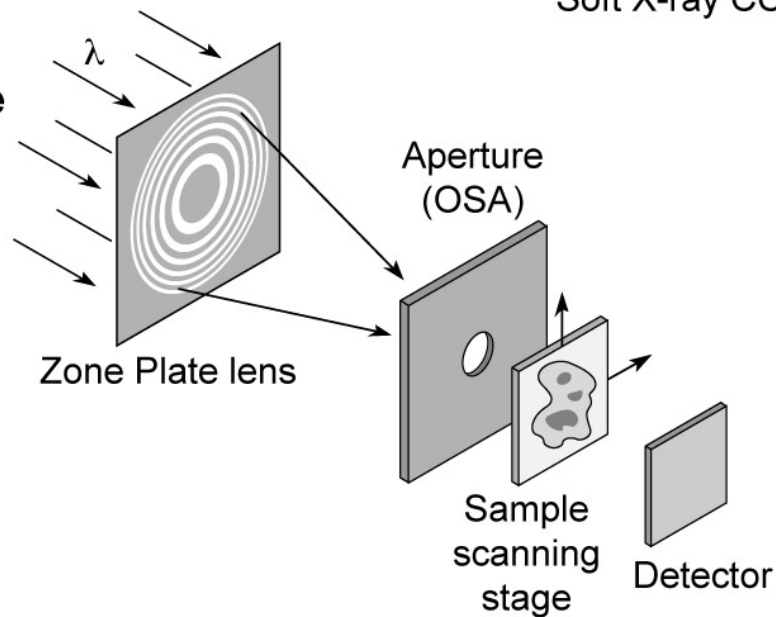
# Two common soft x-ray microscopes

## Full-Field Microscope



- Spatial resolution: 10 nm
- Spectral resolution: 5,000
- Shortest exposure time: 1 sec.
- Bending magnet radiation
- Higher radiation dose
- Flexible sample environment (wet, cryo, labeled magnetic fields, electric fields, cement, ...)

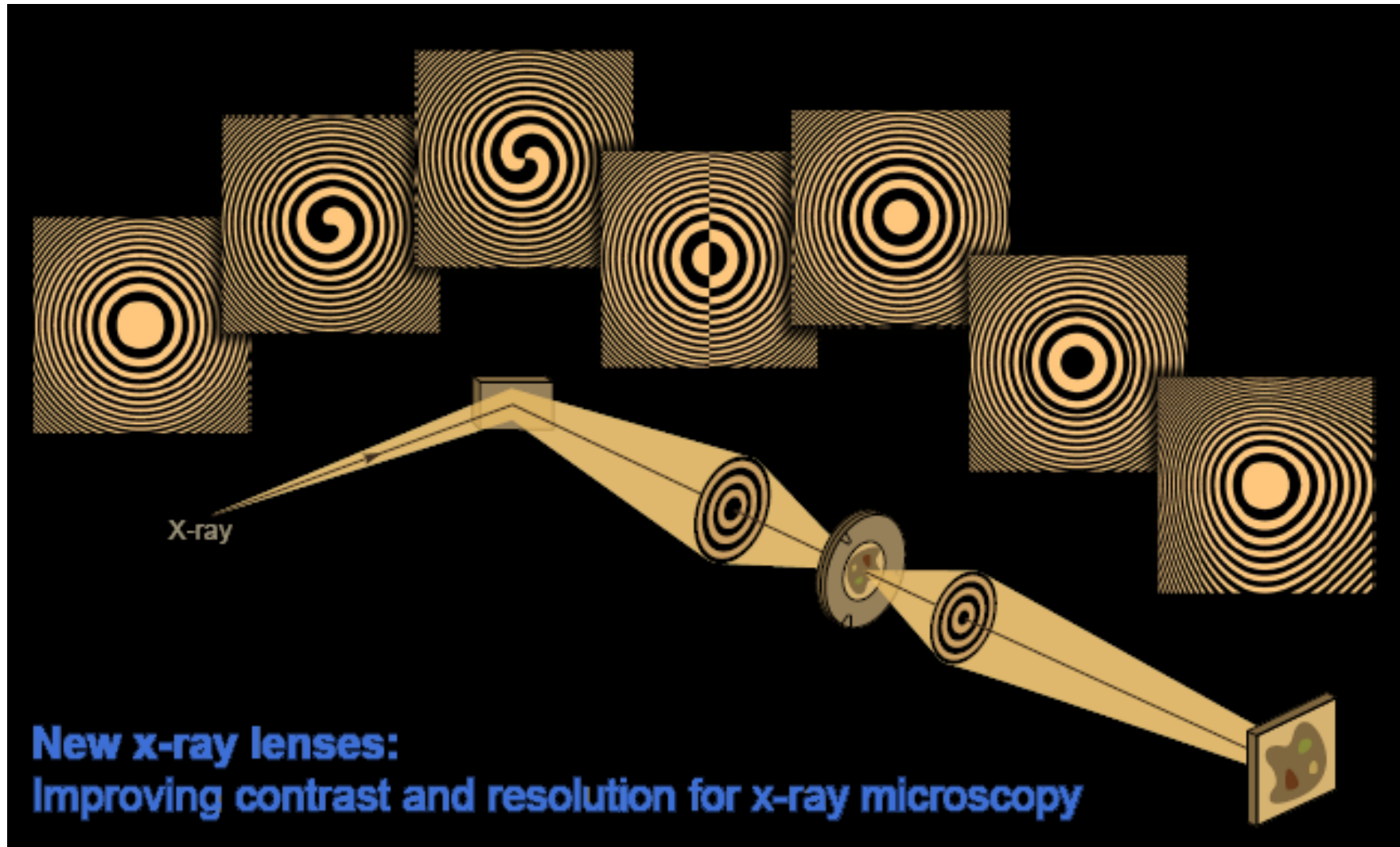
## Scanning Microscope



- Least radiation dose
- Spatial resolution: 10 nm
- Spectral resolution: 5,000
- Requires undulator, spatially coherent radiation
- Long exposure time
- Flexible sample environment

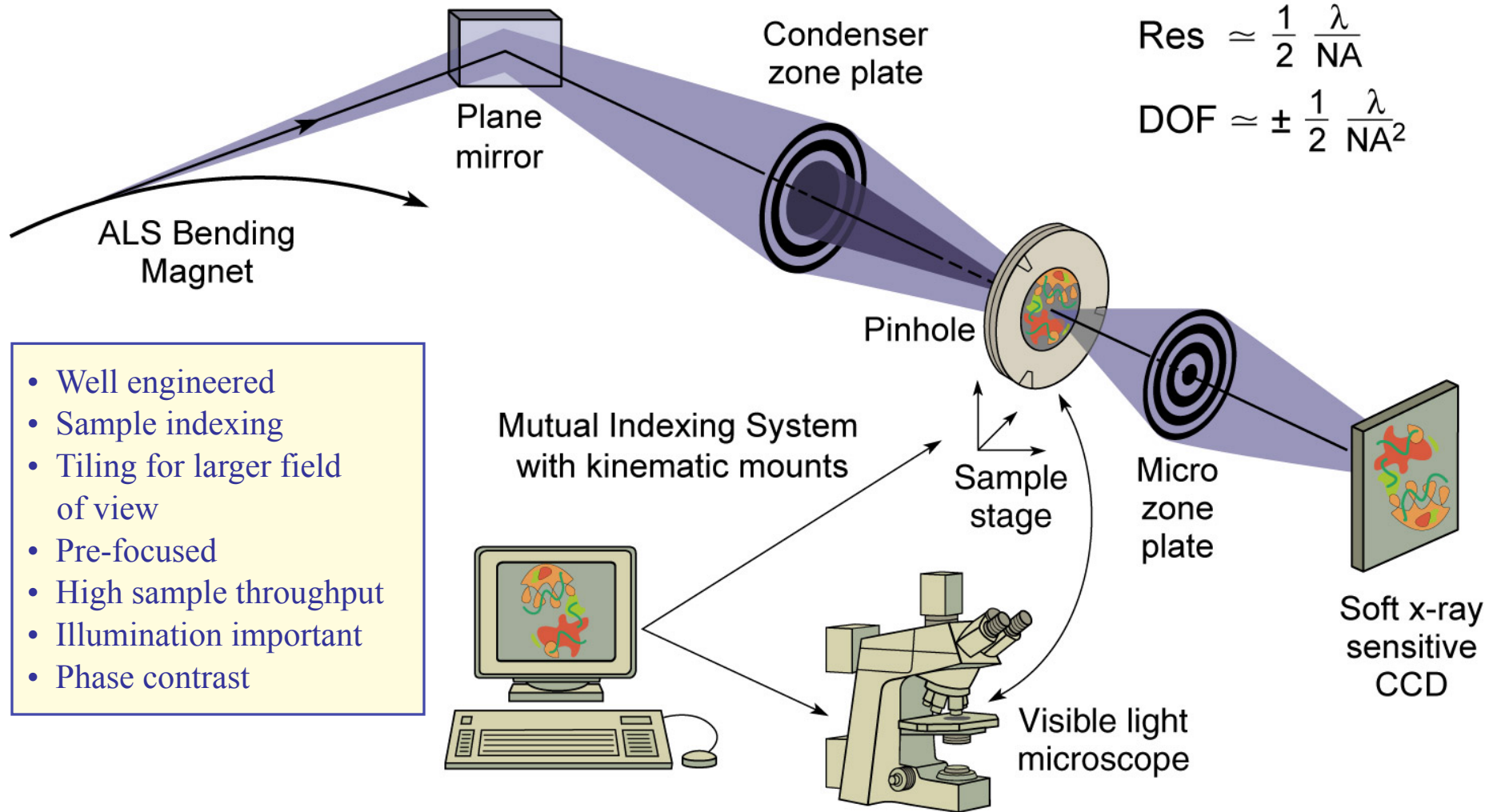


# Novel zone plates for specific functionality



Courtesy of Anne Sakdinawat, UC Berkeley

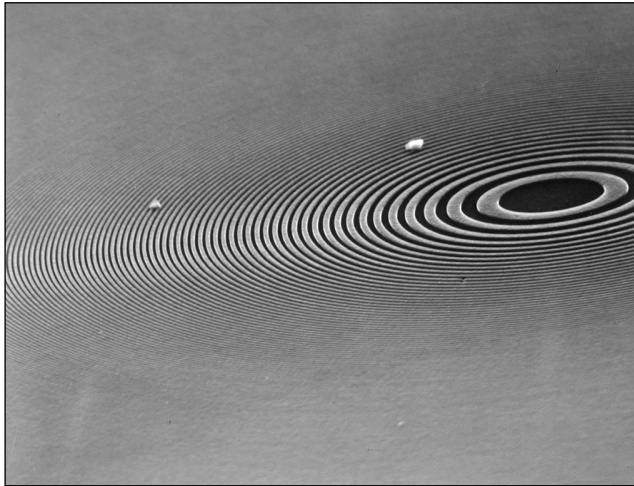
# High resolution zone plate microscopy



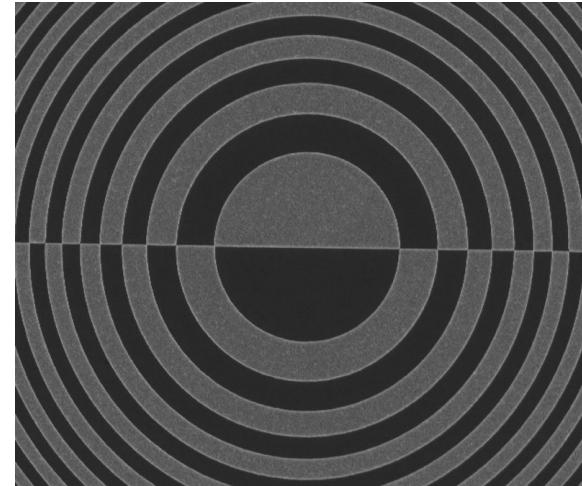
HiResZPMicrXM1Biology\_Jan08.ai



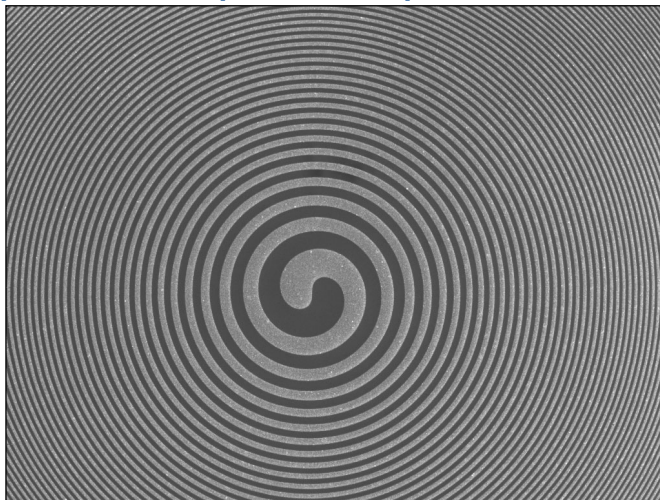
Soft x-ray zone plate



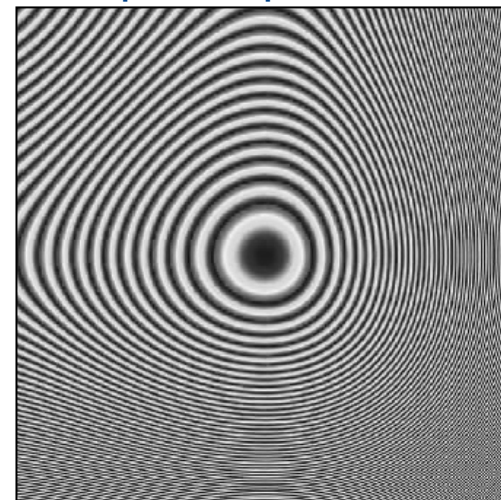
DIC microscopy



Spiral zone plate for phase contrast

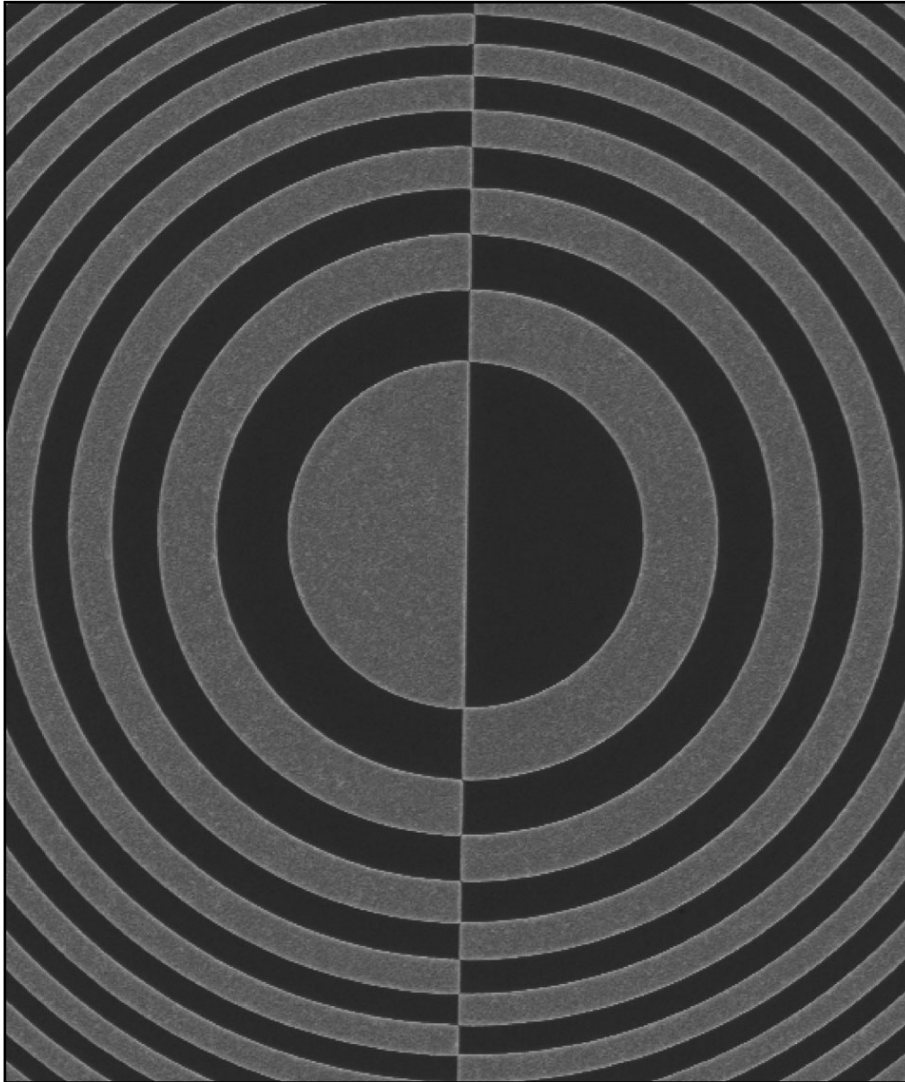


Cubic phase plate for DOF

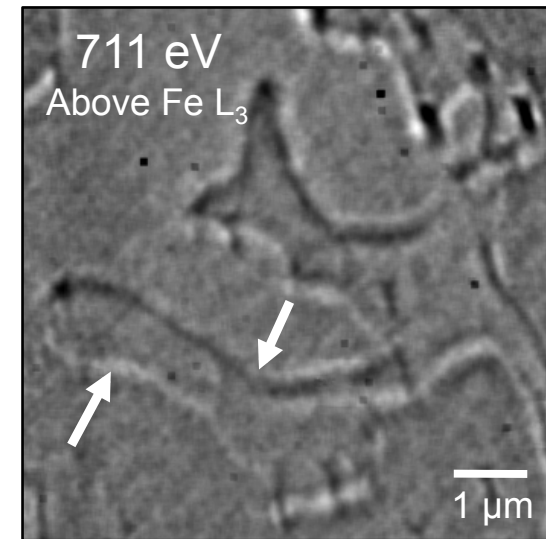
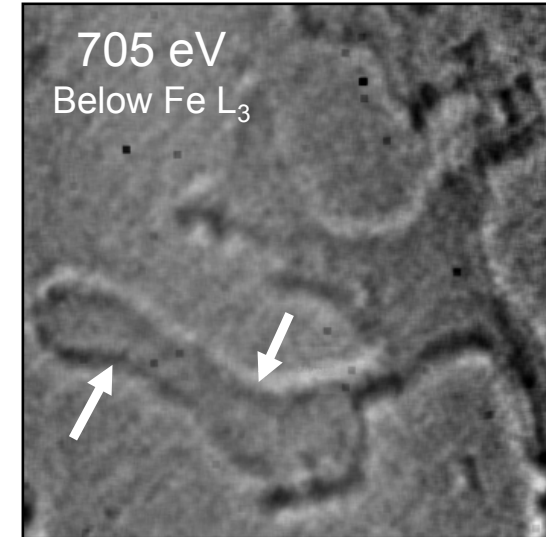


*Courtesy of Anne Sakdinawat, Chang Chang, Weilun Chao and Erik Anderson (LBNL & UCB.)*

# Differential interference contrast (DIC) imaging at nanoscale magnetic edges



XOR Zone plate



59 nm thick Gd<sub>25</sub>Fe<sub>75</sub> layer

Courtesy of A. Sakdinawat, C. Chang and P. Fischer.



# Soft X-ray microscopy at a spatial resolution better than 15 nm

Weilun Chao<sup>1,2</sup>, Bruce D. Harteneck<sup>1</sup>, J. Alexander Liddle<sup>1</sup>, Erik H. Anderson<sup>1</sup> & David T. Attwood<sup>1,2</sup>

Analytical tools that have spatial resolution at the nanometre scale are indispensable for the life and physical sciences. It is desirable that these tools also permit elemental and chemical identification on a scale of 10 nm or less, with large penetration depths. A variety of techniques<sup>1–7</sup> in X-ray imaging are currently being developed that may provide these combined capabilities. Here we report the achievement of sub-15-nm spatial resolution with a soft X-ray microscope—and a clear path to below 10 nm—using an overlay technique for zone plate fabrication. The microscope covers a spectral range from a photon energy of 250 eV (~5 nm wavelength) to 1.8 keV (~0.7 nm), so that primary K and L atomic resonances of elements such as C, N, O, Al, Ti, Fe, Co and Ni can be probed. This X-ray microscopy technique is therefore suitable for a wide range of studies: biological imaging in the water window<sup>8,9</sup>; studies of wet environmental samples<sup>10,11</sup>; studies of magnetic nanostructures with both elemental and spin-orbit sensitivity<sup>12–14</sup>; studies that require viewing through thin windows, coatings or substrates (such as buried electronic devices in a silicon chip<sup>15</sup>); and three-dimensional imaging of cryogenically fixed biological cells<sup>9,16</sup>.

The microscope XM-1 at the Advanced Light Source (ALS) in Berkeley<sup>17</sup> is schematically shown in Fig. 1. The microscope type is similar to that pioneered by the Göttingen/BESSY group (ref. 18, and references therein). A ‘micro’ zone plate (MZP) projects a full-field image to an X-ray-sensitive CCD (charge-coupled device), typically in one or a few seconds, often with several hundred images per day. The field of view is typically 10  $\mu\text{m}$ , corresponding to a magnification of 2,500. The condenser zone plate (CZP), with a central stop, serves two purposes in that it provides partially coherent hollow-cone illumination<sup>2</sup>, and, in combination with a pinhole, serves as the

monochromator. Monochromatic radiation of  $\lambda/\Delta\lambda = 500$  is used. Both zone plates are fabricated in-house, using electron beam lithography<sup>19</sup>.

The spatial resolution of a zone plate based microscope is equal to  $k_1\lambda/NA_{MZP}$ , where  $\lambda$  is the wavelength,  $NA_{MZP}$  is the numerical aperture of the MZP, and  $k_1$  is an illumination dependent constant, which ranges from 0.3 to 0.61. For a zone plate lens used at high magnification,  $NA_{MZP} = \lambda/2\Delta r_{MZP}$ , where  $\Delta r_{MZP}$  is the outermost (smallest) zone width of the MZP<sup>20</sup>. For the partially coherent illumination<sup>21,22</sup> used here,  $k_1 \approx 0.4$  and thus the theoretical resolution is  $0.8\Delta r_{MZP}$ , as calculated using the SPLAT computer program<sup>23</sup> (a two-dimensional scalar diffraction code, which evaluates partially coherent imaging). In previous results with a  $\Delta r_{MZP} = 25$  nm zone plate, we reported<sup>2</sup> an unambiguous spatial resolution of 20 nm. Here we describe the use of an overlay nanofabrication technique that allows us to fabricate zone plates with finer outer zone widths, to  $\Delta r_{MZP} = 15$  nm, and to achieve a spatial resolution of below 15 nm, with clear potential for further extension.

This technique overcomes nanofabrication limits due to electron beam broadening in high feature density patterning. Beam broadening results from electron scattering within the recording medium (resist), leading to a loss of image contrast and thus resolvability for

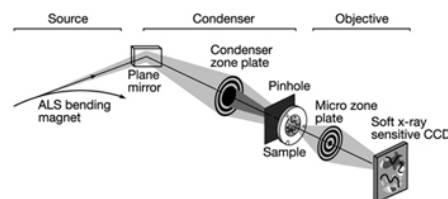


**Figure 1** | A diagram of the soft X-ray microscope XM-1. The microscope uses a micro zone plate to project a full field image onto a CCD camera that is sensitive to soft X-rays. Partially coherent, hollow-cone illumination of the sample is provided by a condenser zone plate. A central stop and a pinhole provide monochromatization.

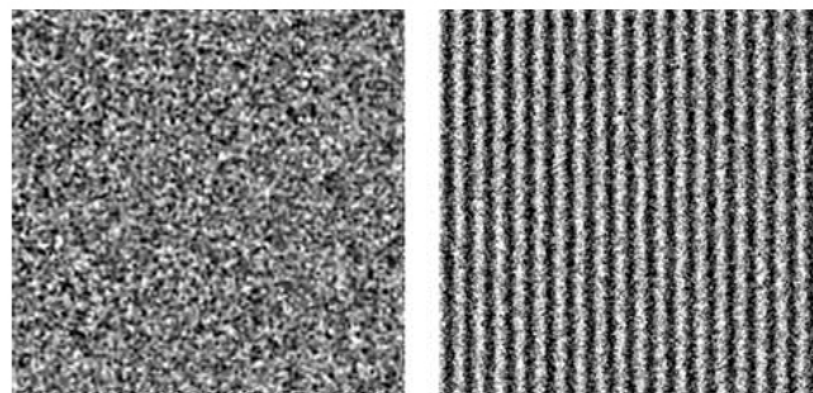
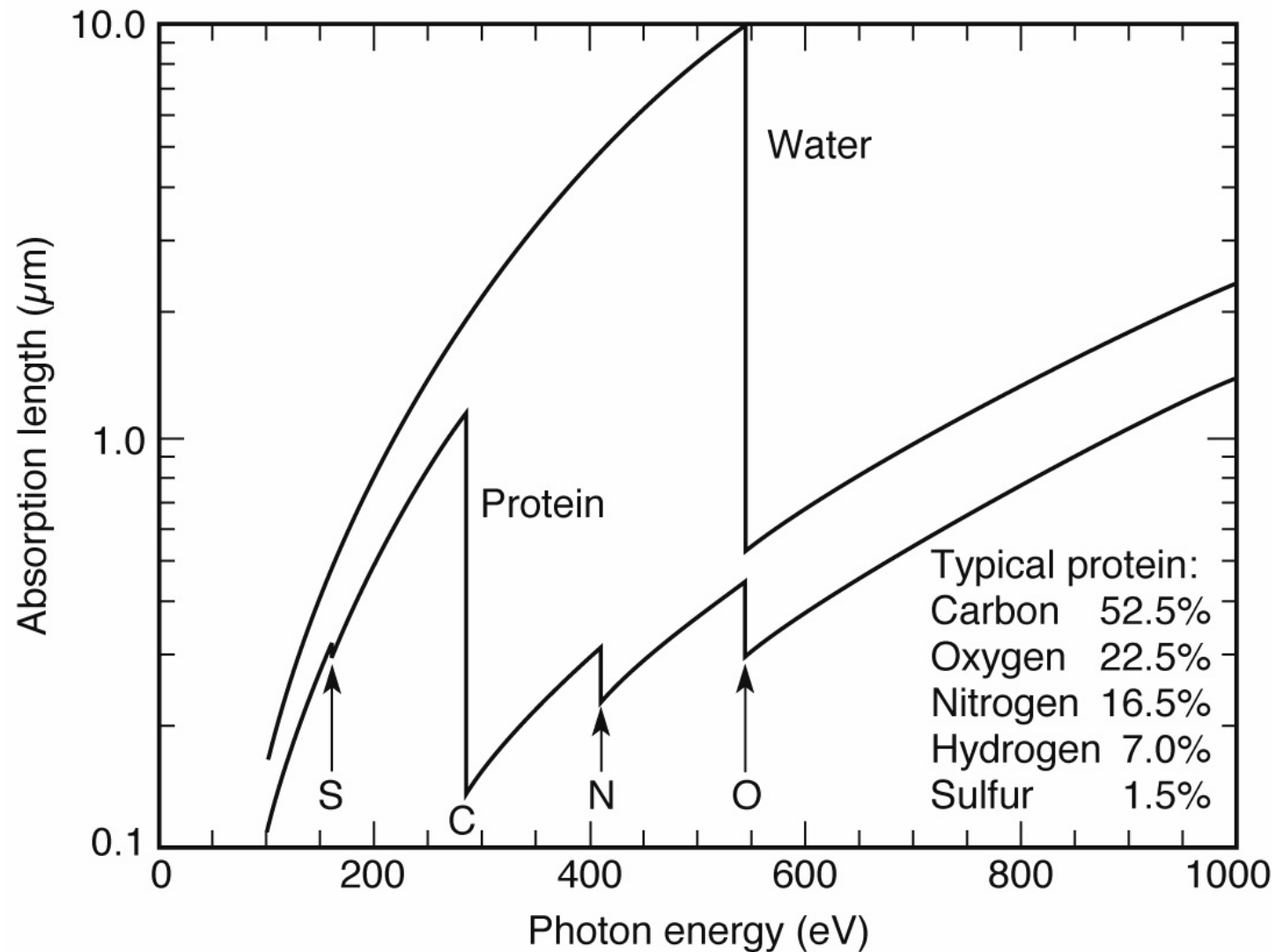


**Figure 4** | Soft X-ray images of a 15.1 nm half-period test object, as formed with zone plates having outer zone widths of 25 nm and 15 nm.

Cr/Si test pattern (Cr L<sub>3</sub> @ 574 eV)  
(2000 X 2000, 10<sup>4</sup> ph/pixel)

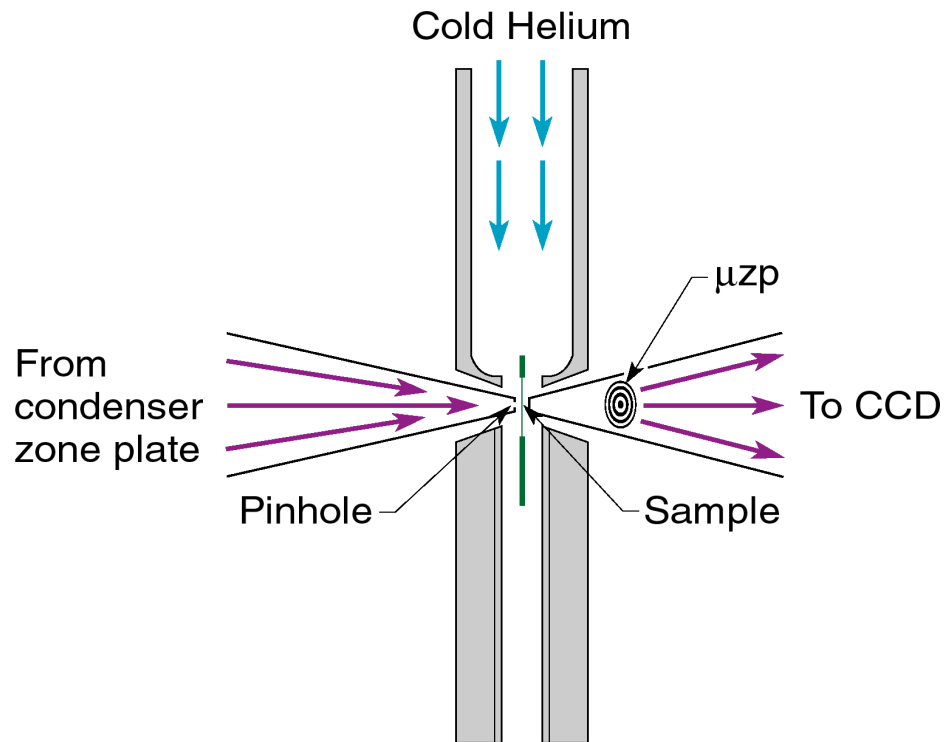
<sup>1</sup>Center for X-ray Optics, Lawrence Berkeley National Laboratory, 1 Cyclotron Road, MS 2-400, <sup>2</sup>Department of Electrical Engineering, California, Berkeley, California 94720, USA.

# The water window for biological x-ray microscopy



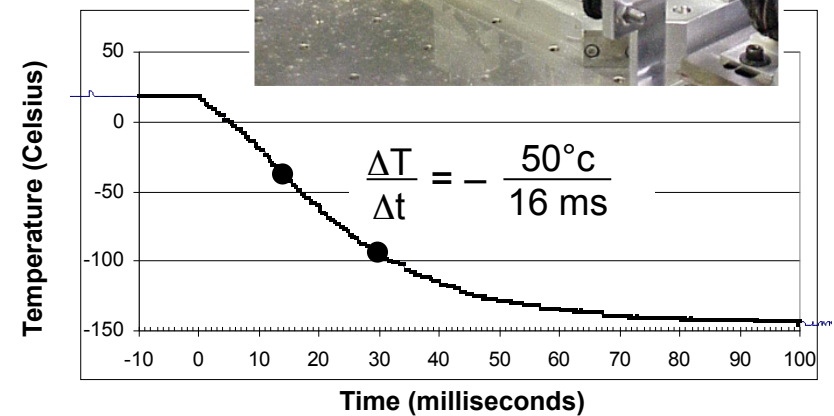
Ch09\_F25VG.ai

# Fast freeze cryo fixation strongly mitigates radiation dose effects



Helium passes through LN, is cooled, and directed onto sample windows

Fast Freeze

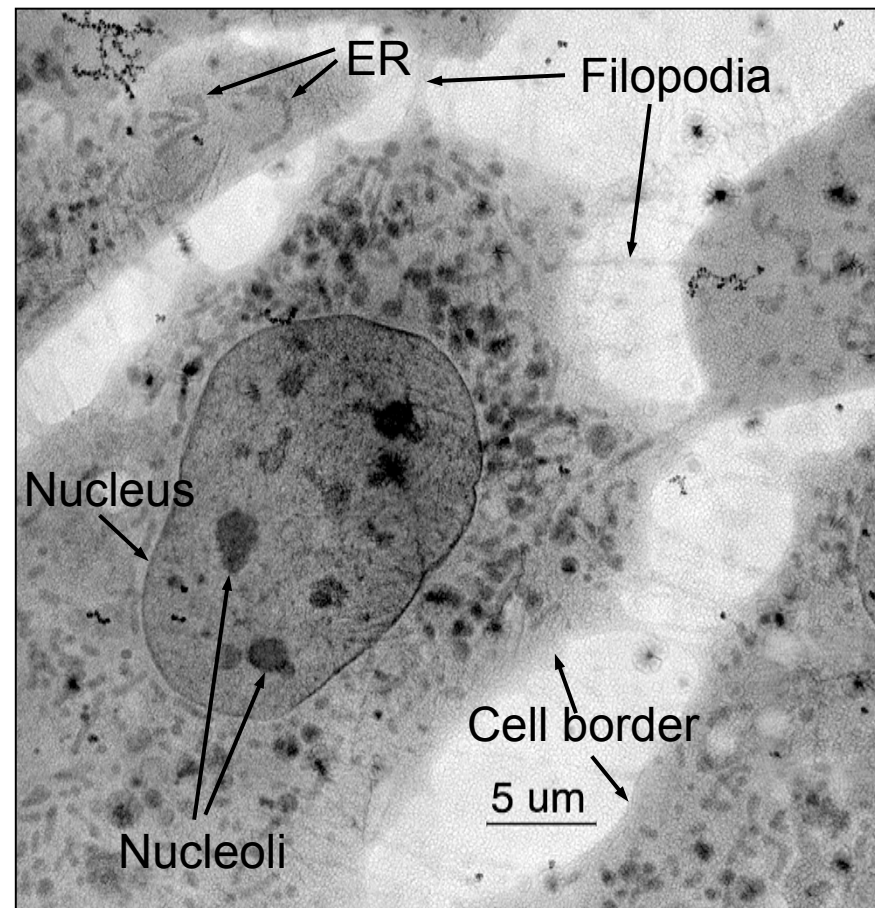


W. Meyer-Ilse, G. Denbeaux, L. Johnson, A. Pearson (CXRO-LBNL)



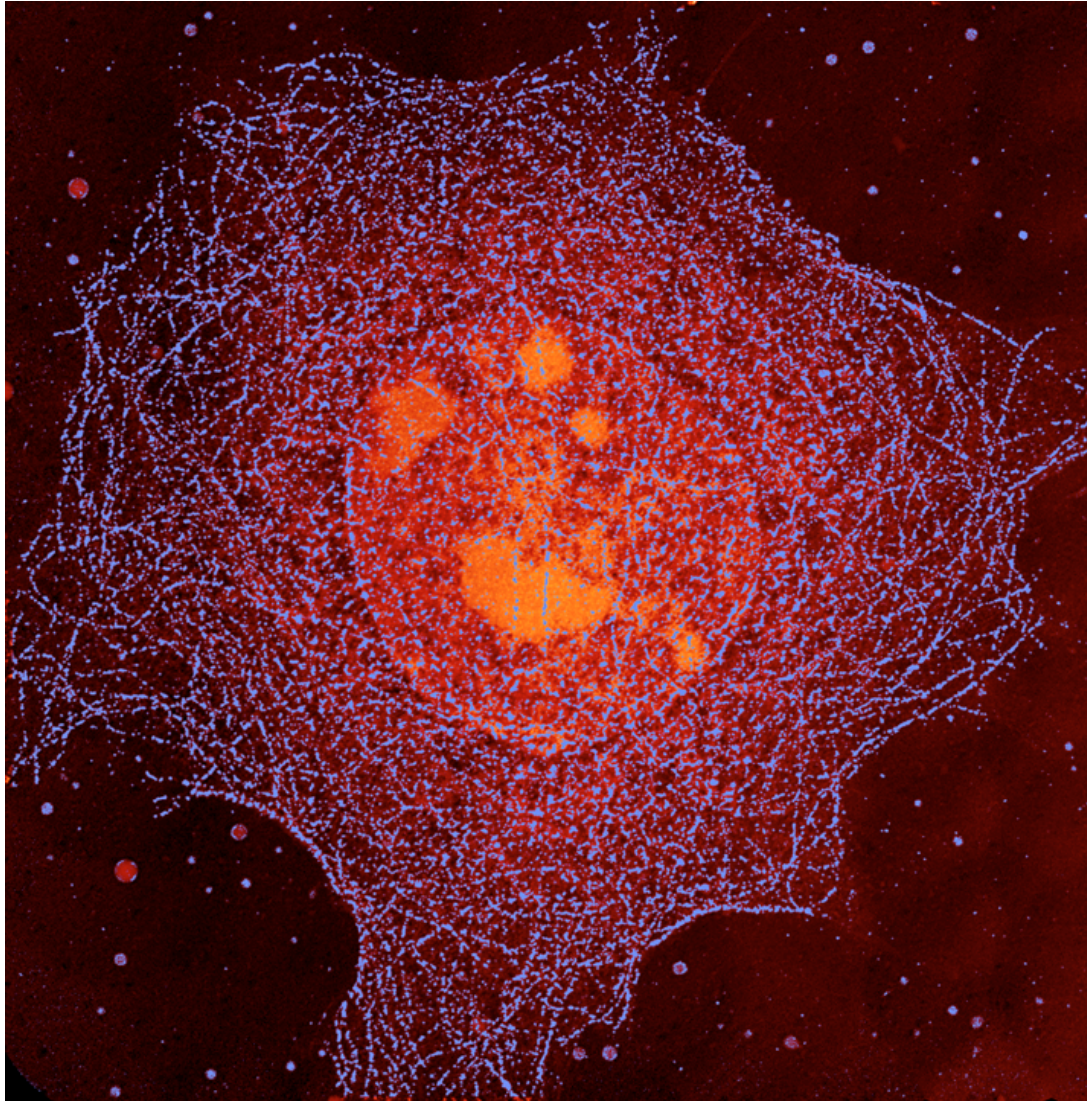
# Organelle details imaged with cryogenic preservation and high spatial resolution

## Cryo x-ray microscopy of 3T3 fibroblast cells



C. Larabell, D. Yager, D. Hamamoto, M. Bissell, T. Shin (LBNL Life Sciences Division)  
W. Meyer-Ilse, G. Denbeaux, L. Johnson, A. Pearson (CXRO-LBNL)

## Bending magnet radiation used with a soft x-ray microscope to form a high resolution image of a whole, hydrated mouse epithelial cell



$\hbar\omega = 520 \text{ eV}$

$32 \mu\text{m} \times 32 \mu\text{m}$

Ag enhanced Au labeling  
of the microtubule network,  
color coded blue.

Cell nucleus and nucleoli,  
moderately absorbing,  
coded orange.

Less absorbing aqueous  
regions coded black.

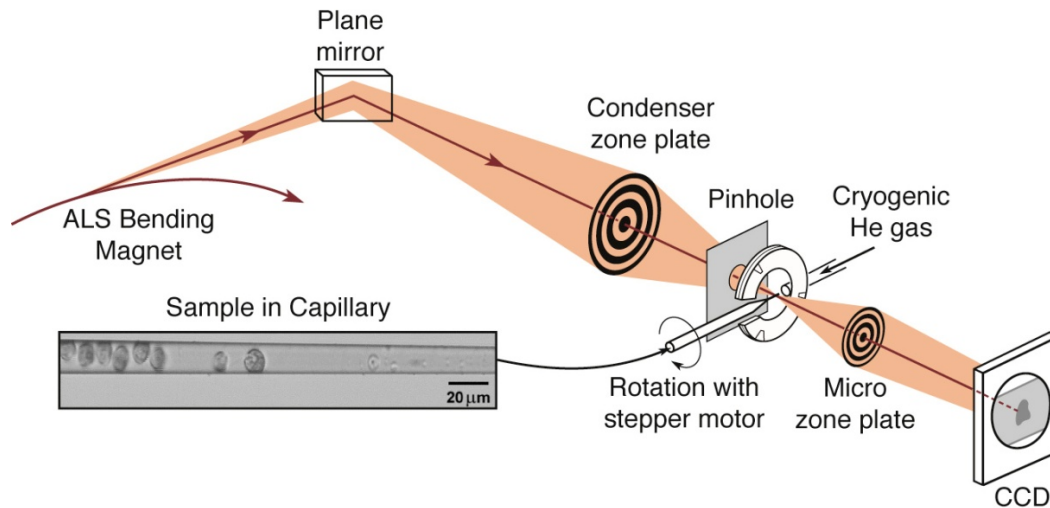
W. Meyer-Ilse et al.

J. Microsc. 201, 395 (2001)

Courtesy of C. Larabell and W. Meyer-Ilse (LBNL)

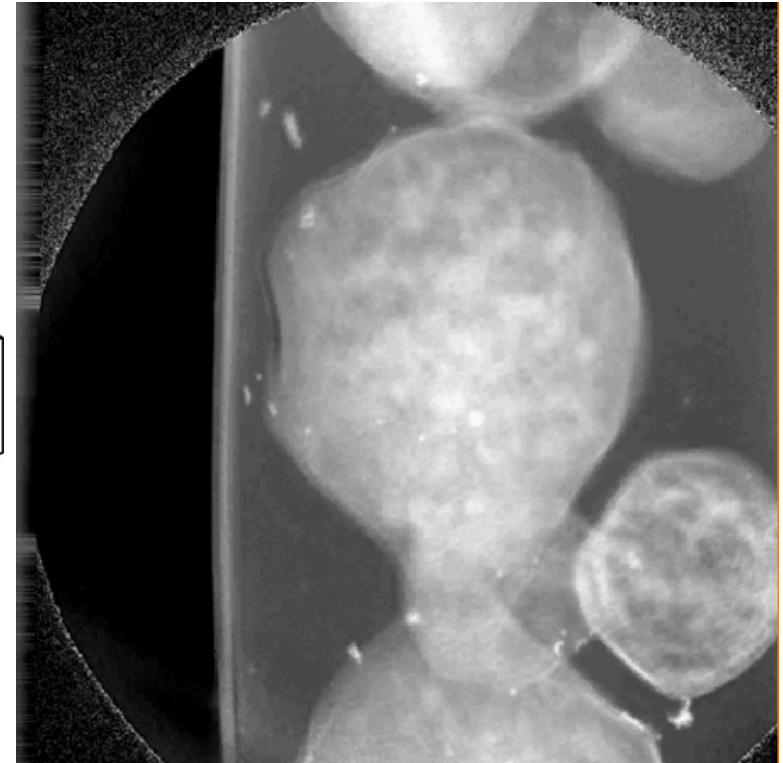


## Nanotomography of Cryogenic Fixed Cells



Courtesy of G. Schneider (BESSY)  
*Surf. Rev. Lett.* **9**, 177 (2002)

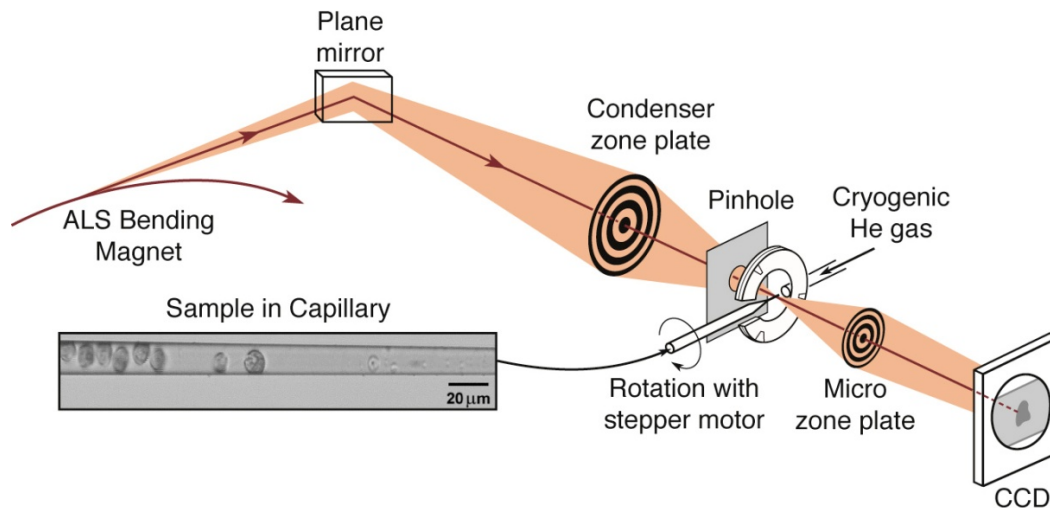
## Soft X-Ray Nanotomography of a Yeast Cell



$\lambda = 2.4 \text{ nm}$

Courtesy of C. Larabell (UCSF & LBNL)  
 and M. LeGros (LBNL)

## Nanotomography of Cryogenic Fixed Cells



$$\lambda = 2.4 \text{ nm (517 eV)}$$

$$\Delta r = 35 \text{ nm}$$

$$N = 320$$

$$NA = 0.034$$

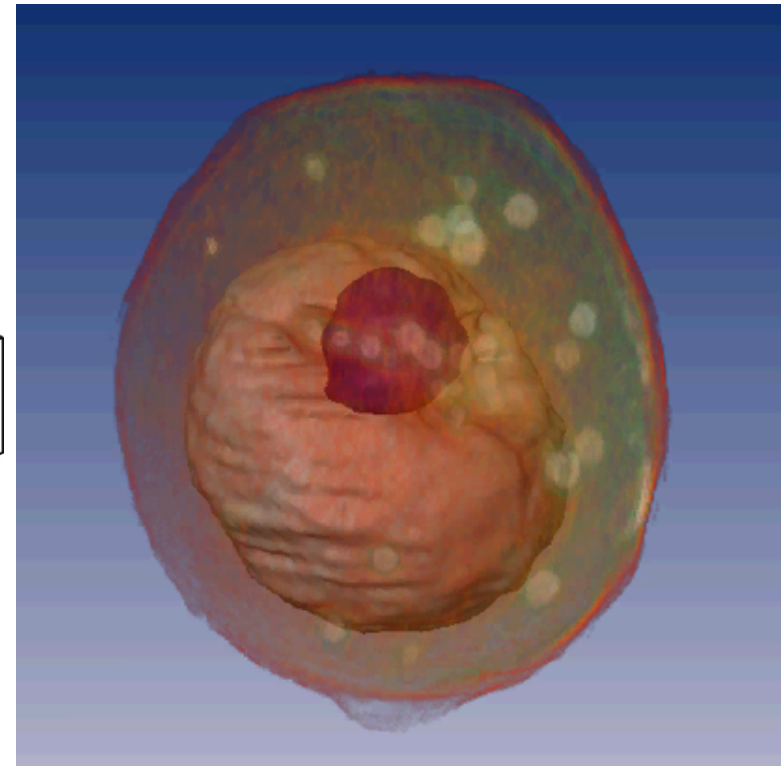
$$D = 45 \mu\text{m}$$

$$f = 650 \mu\text{m}$$

$$\sigma = 0.64$$

$$\text{Resolution} = 60 \text{ nm}$$

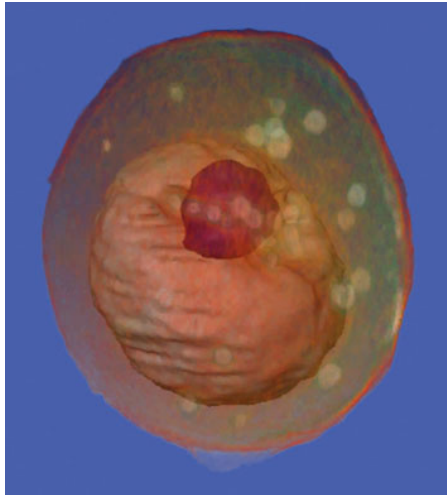
## Soft X-Ray Nanotomography of a Yeast Cell



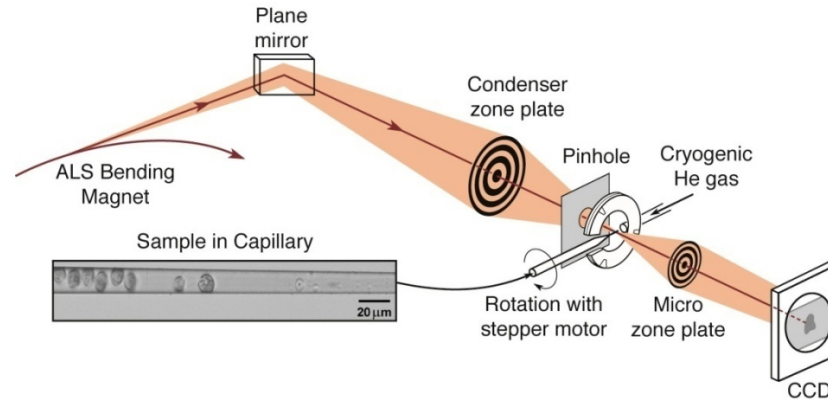
$$\lambda = 2.4 \text{ nm}$$

Courtesy of C. Larabell (UCSF & LBNL)  
and M. LeGros (LBNL)

# Small DOF limits resolution for thick samples



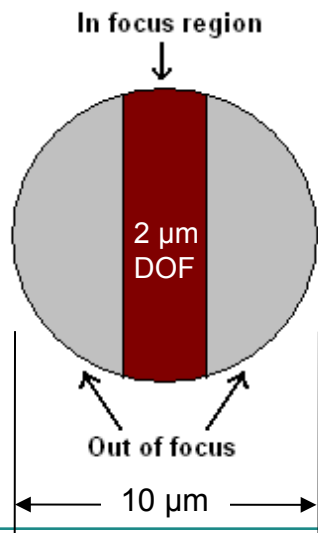
C. Larabell and M. LeGros,  
*Molec. Bio. Cell* 15, 957 (2004)



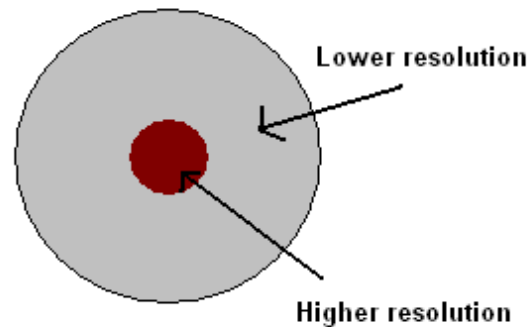
$$\text{Lateral Resolution} = \frac{k_1 \lambda}{NA} = 2k_1 \Delta r = \cancel{28 \text{ nm}} \quad 60 \text{ nm}$$

$$\text{Depth of field} = 2 \mu\text{m}$$

## Each projection image



## Reconstructed image



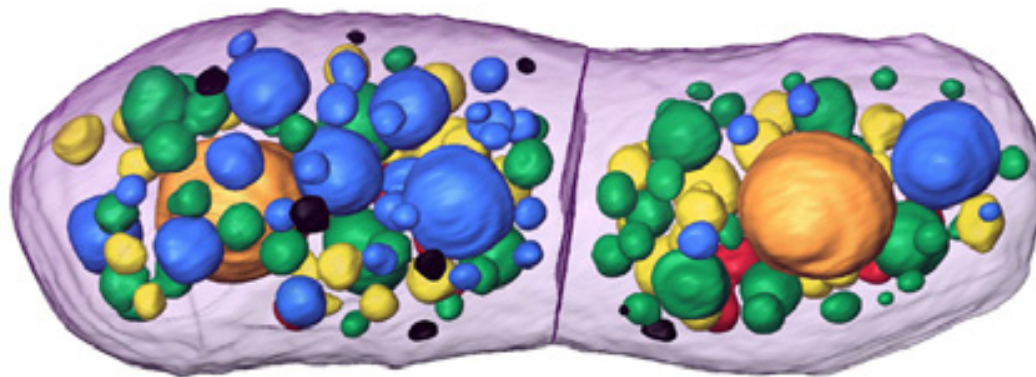
*Courtesy of Anne Sakdinawat (LBNL & UCB.)*

# Nanoscale 3-D biotomography

Mother daughter yeast cells just before separation



2-D slice from 3-D Tomogram. Images every 2°, 180° data set, several minutes.  $\Delta r = 45$  nm

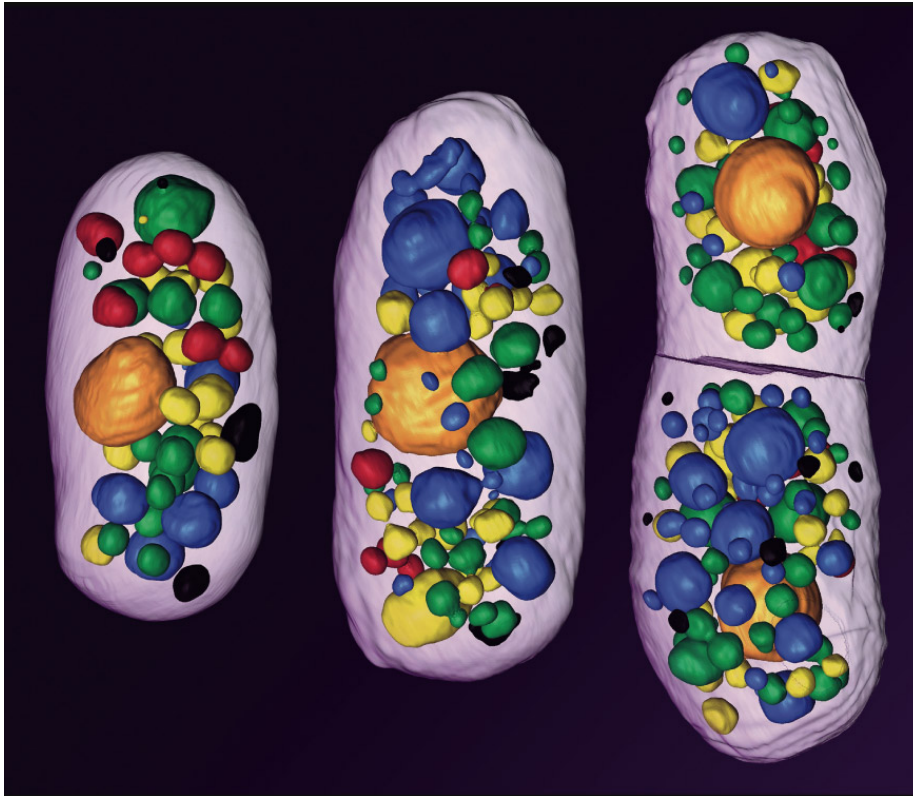


Color coding identifies subcellular components by their x-ray absorption coefficients

Courtesy of Carolyn Larabell, UCSF/LBNL.



## Biotomography at 60 nm resolution

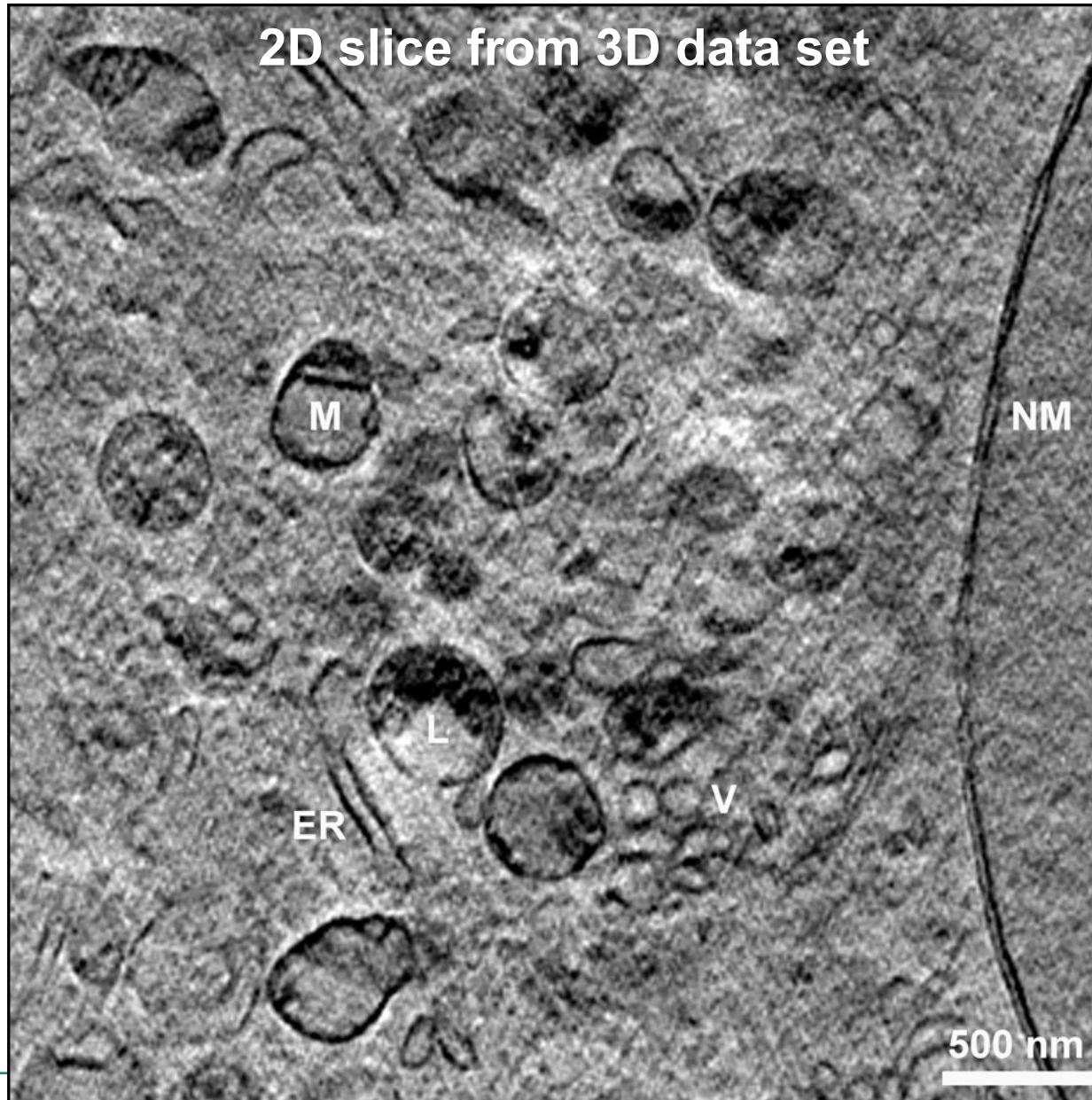


- Cryofixation
- 2° angular intervals
- Depth of focus limits resolution
- New XM-2 dedicated to biological applications, will become major facility worldwide to draw biologists to this evolving capability

Courtesy of C. Larabell (UCSF & LBNL)

UCSF NCXT

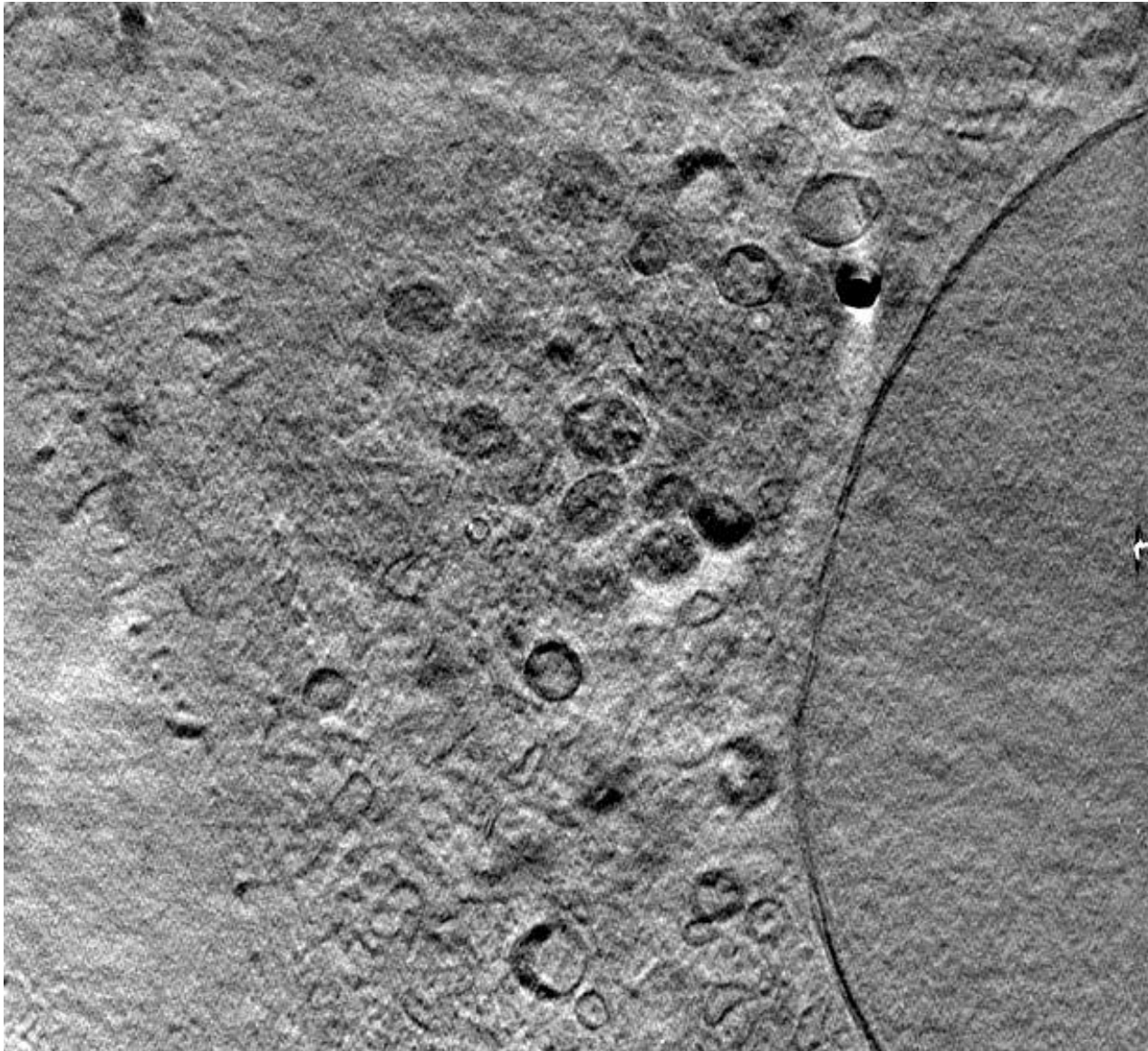
# High resolution 3D image of a mouse cell by soft x-ray tomography



517 eV (2.4 nm)  
 $\Delta r = 25$  nm,  
1° intervals,  $\pm 60^\circ$   
29 nm nuclear  
double membrane.

Courtesy of  
Gerd Schneider, BESSYII  
and James McNally, NIH.





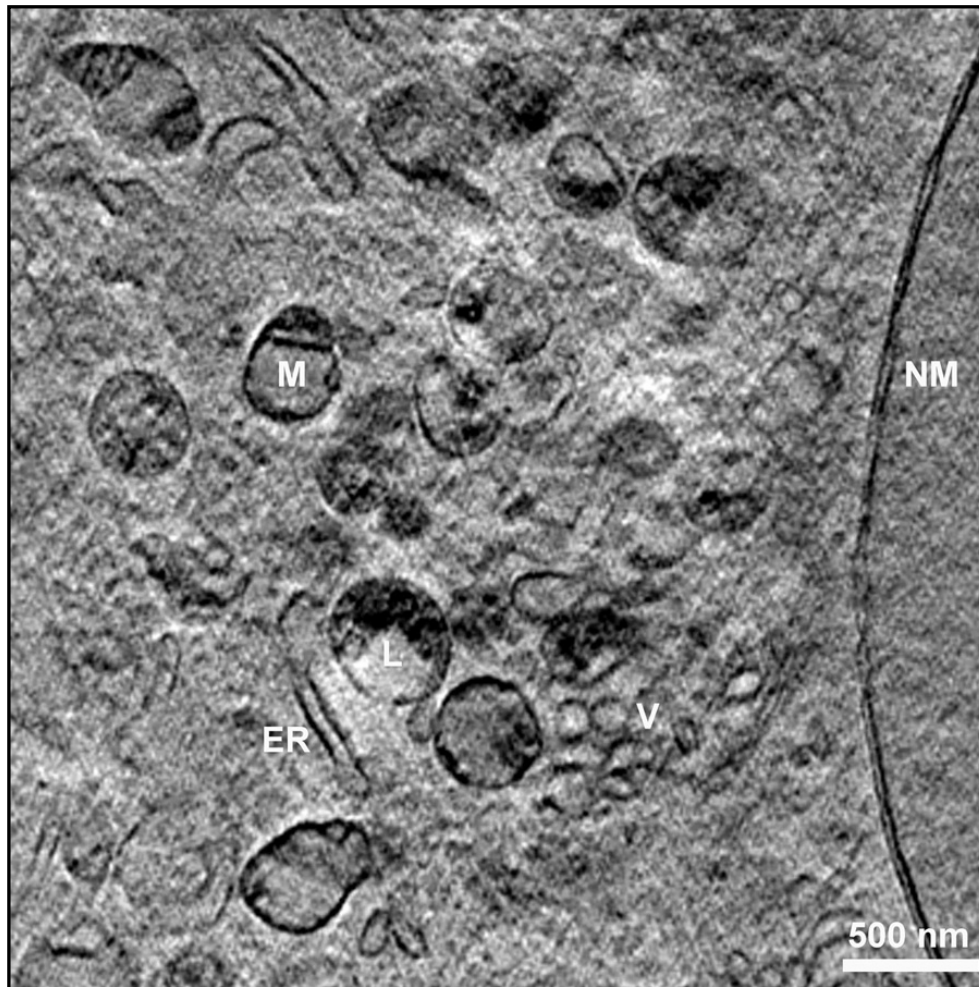
517 eV (2.4 nm)  
 $\Delta r = 25$  nm,  
1° intervals,  $\pm 60^\circ$   
29 nm nuclear  
double membrane.

Courtesy of  
Gerd Schneider,  
BESSYII and  
James McNally, NIH.



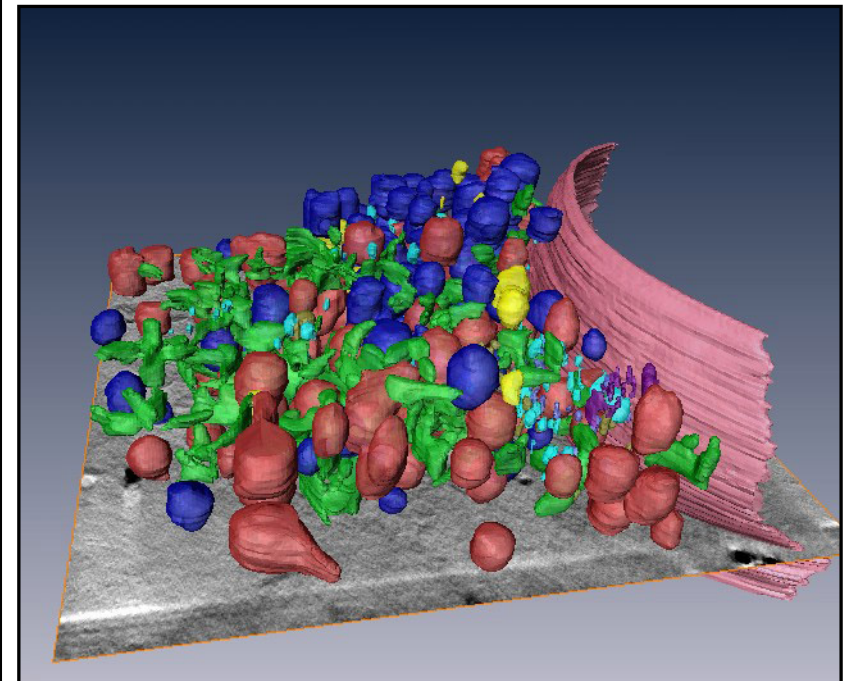
# High resolution 3D image of a mouse cell by soft x-ray tomography

2D slice from 3D data set



Details: 517 eV (2.4 nm)  
 $\Delta r = 25$  nm,  $1^\circ$  intervals,  $\pm 60^\circ$ .  
Note 29 nm nuclear membrane.

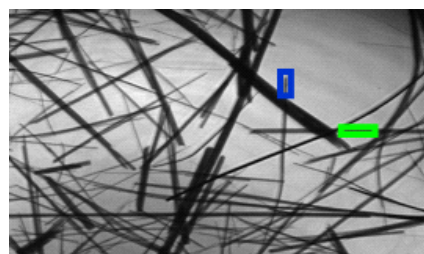
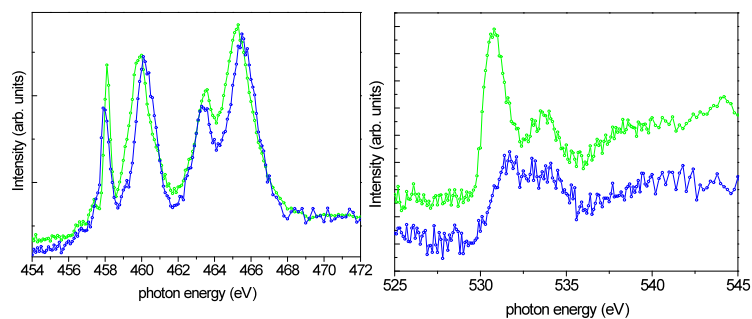
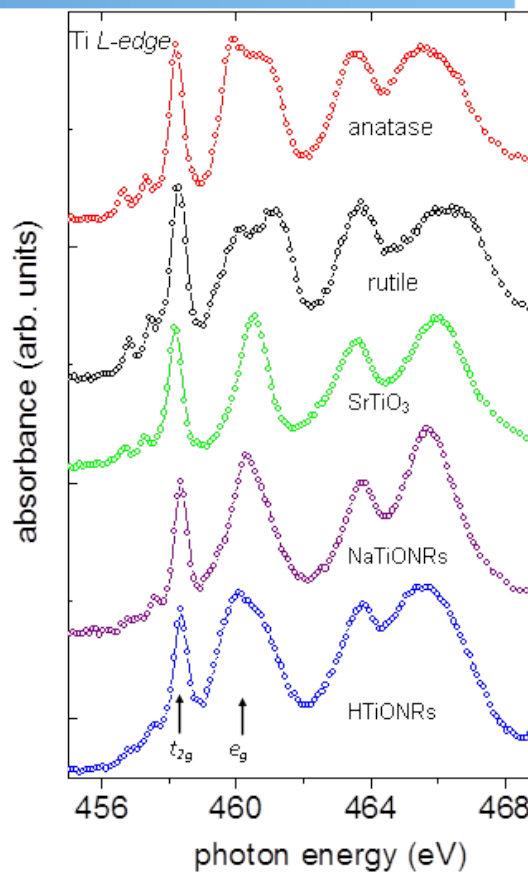
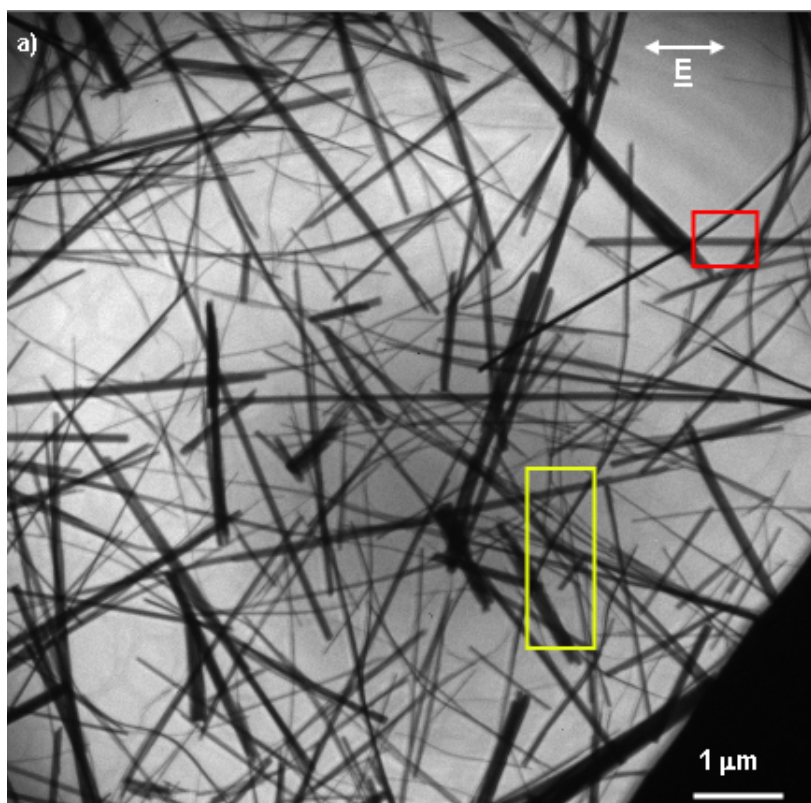
3D rendering



Courtesy of Gerd Schneider, BESSYII and James McNally, NIH.

# Nano-spectroscopy of sodium titanate nanoribbons

In collaboration with:  
C. Bittencourt,  
U. Antwerp, Belgium



P. Guttman et al., *Nature Photonics*  
(Dec. 2011).





# Environmental Consequences of Portland cement

1.5 billion ton of cement

**Problem!**

**Generates 1.5 billion  
ton of CO<sub>2</sub>**

**Responsible for 7%  
CO<sub>2</sub> production in  
the world**

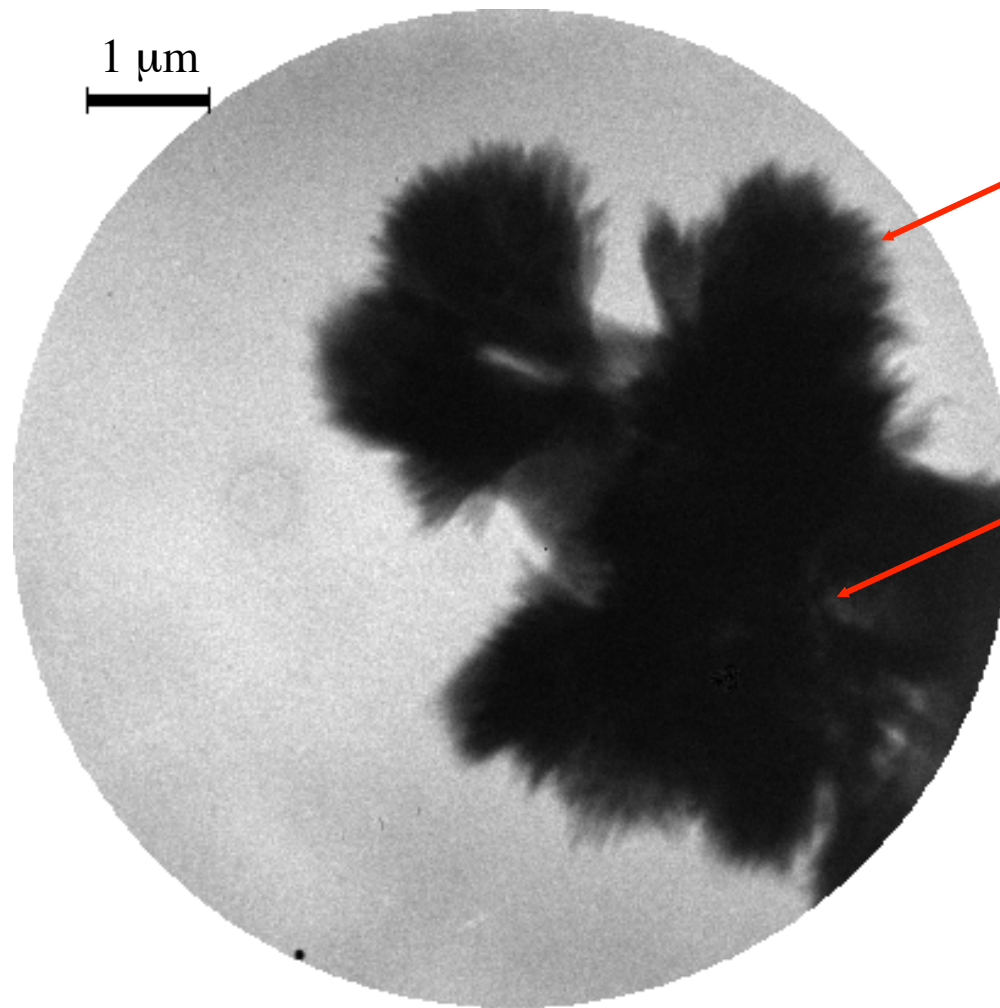


Courtesy of Professor Paulo Monteiro, CEE, UC Berkeley





## Nanoscale x-ray imaging of cement processes: early hydrates forming during the pre-induction period



Early hydrates  
(Sheaf of wheat)

Grain

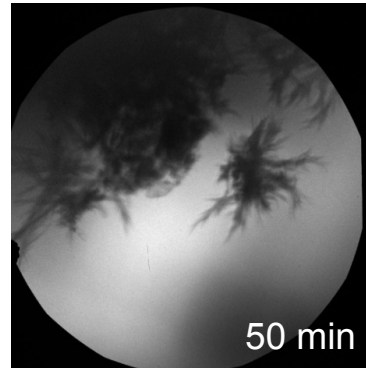
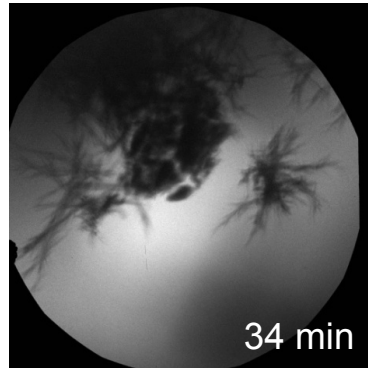
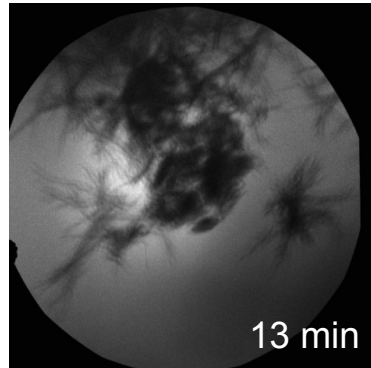
C3S hydrated for 34 min. in  
saturated lime and calcium  
sulfate at  $w/c = 5$ , 1 s  
exposure time, 516 eV, scale  
bar 1 μm.

Courtesy of Professor Paulo Monteiro, CEE, UC Berkeley

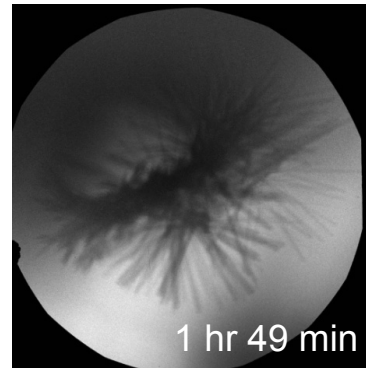
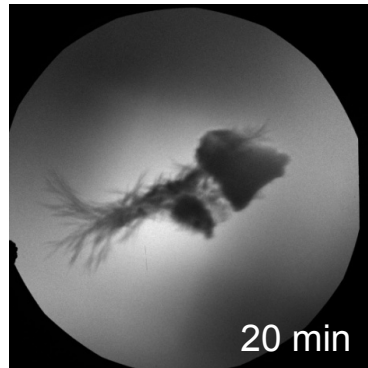
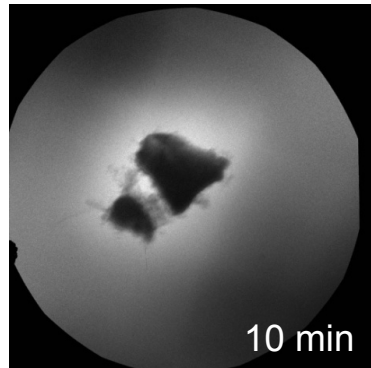


# Nanoscale x-ray imaging of cement processes

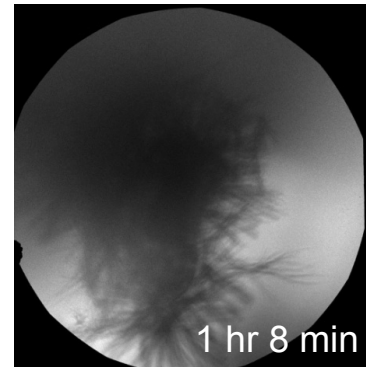
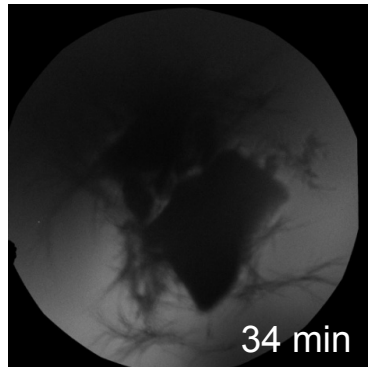
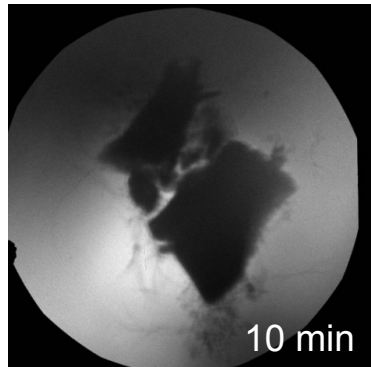
Calcium-Silicate-Hydrate (C-S-H): critical to cement strength and durability.



Orth  $C_3A$



Orth  $C_3A$  + 1%  $CaCl_2$



Orth  $C_3A$  + accelerator

C: carbon

Ca: calcium

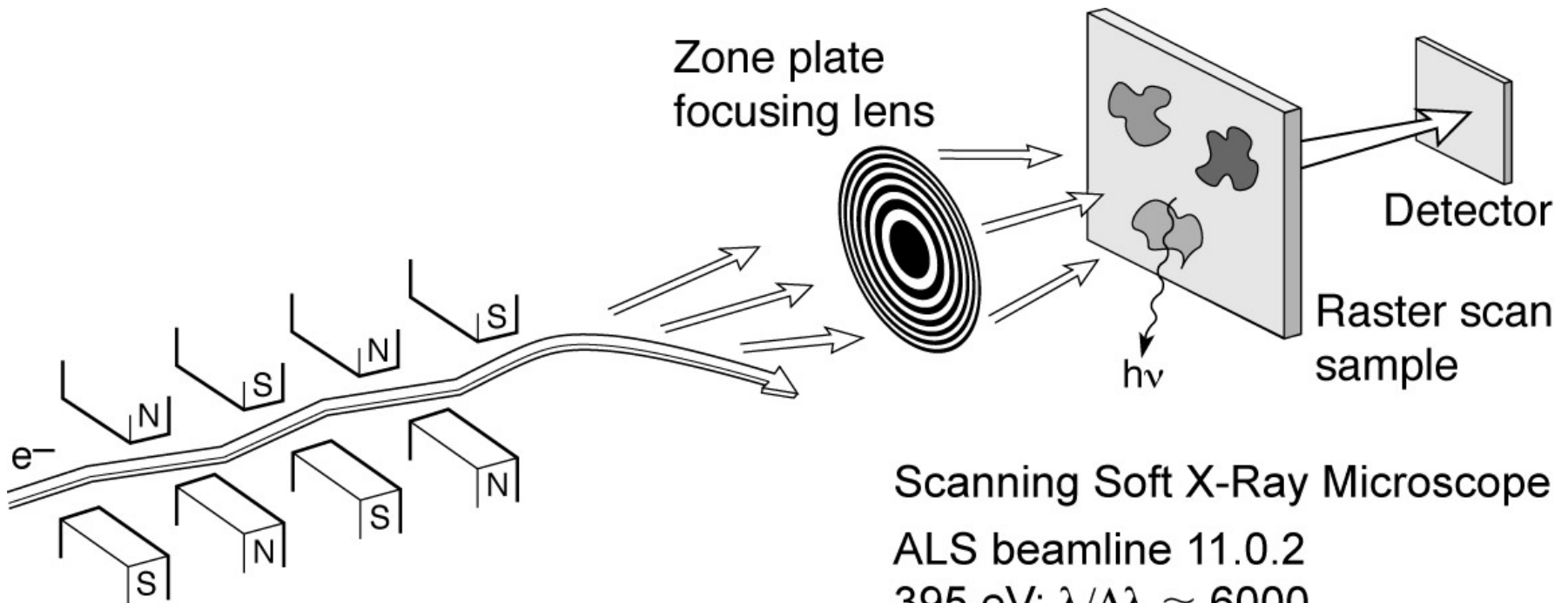
A: alumina ( $Al_2O_3$ )

S: silica ( $SiO_2$ )

520 eV, 40 nm - spatial resolution

Courtesy of Professor Paulo Monteiro, CEE, UC Berkeley

# Spectromicroscopy: high spatial and high spectral resolution of surface and thin films



## Scanning Soft X-Ray Microscope

ALS beamline 11.0.2

395 eV;  $\lambda/\Delta\lambda \approx 6000$

240 × 240 pixels

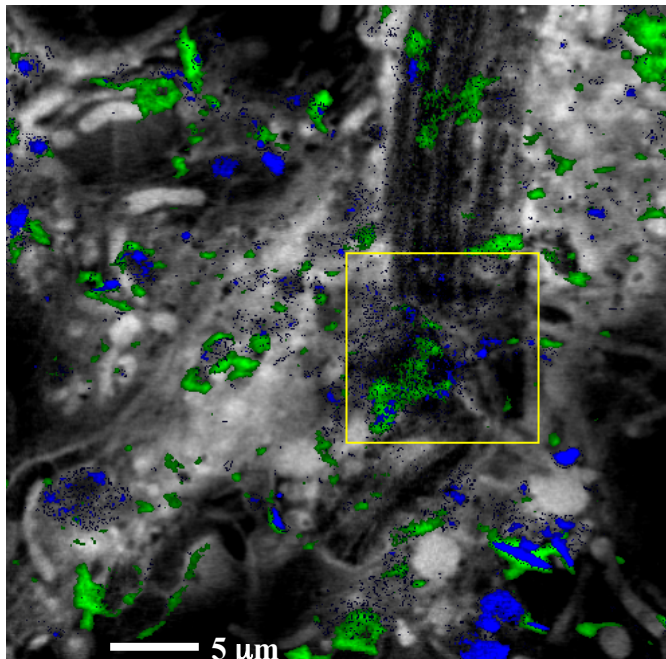
1.2  $\mu\text{m}$  × 1.2  $\mu\text{m}$

2 ms dwell time

Ch09\_F40a\_Feb2010.ai



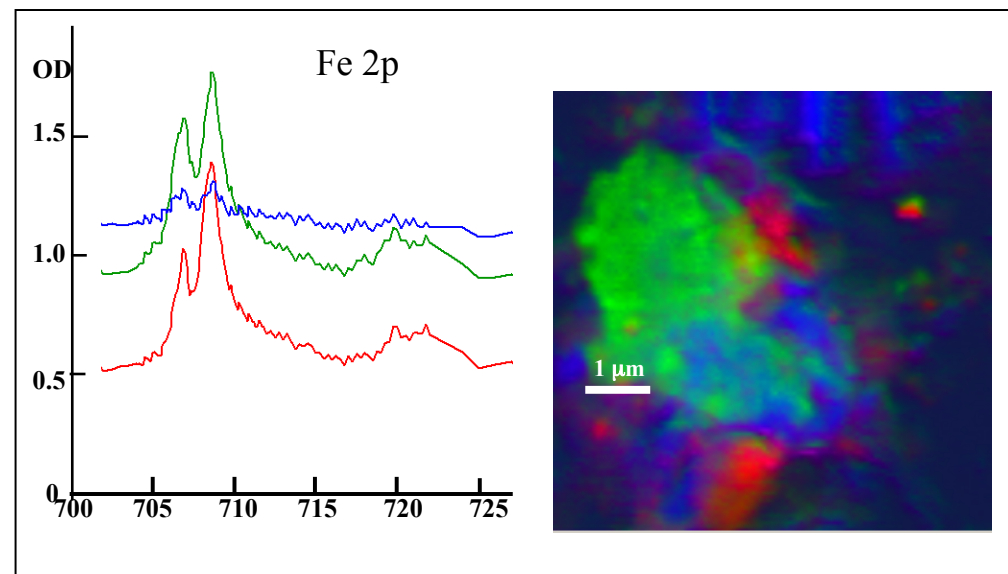
# Biofilm from Saskatoon River



Protein (gray), Ca, K

## RESULTS

- Ni, Fe, Mn, Ca, K, O, C elemental map, (there was no sign of Cr.)
- Different oxidation states for Fe and Ni



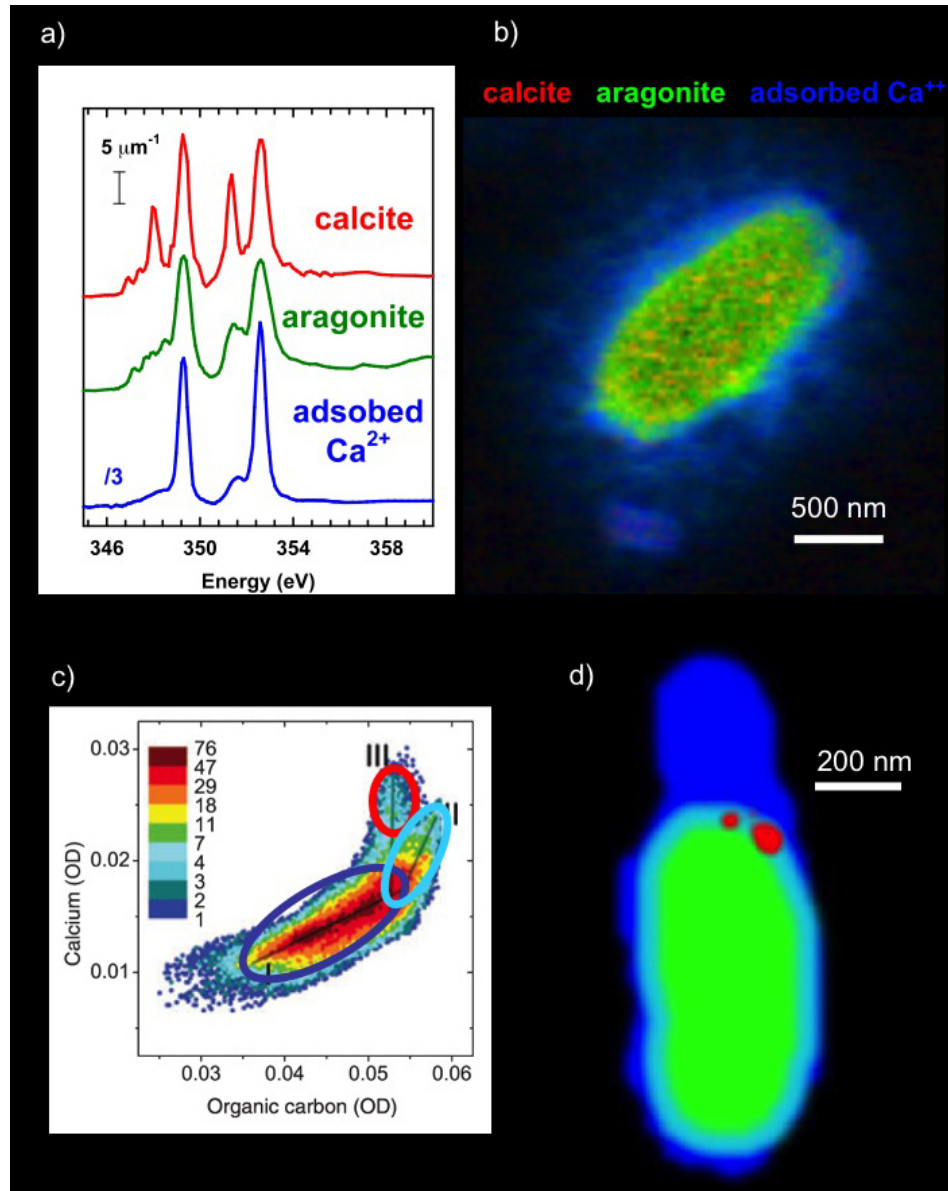
*Different oxidation states (minerals) found for Fe & Ni*

Tohru Araki, Adam Hitchcock (McMaster University)

Tolek Tyliczszak, LBNL

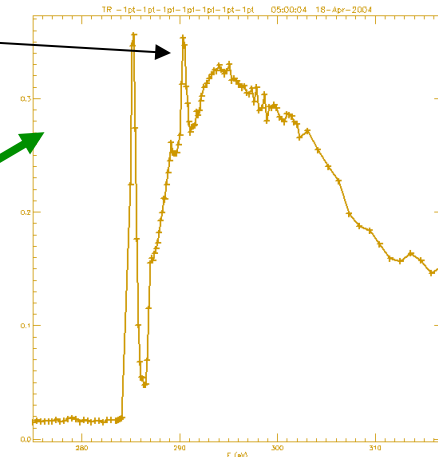
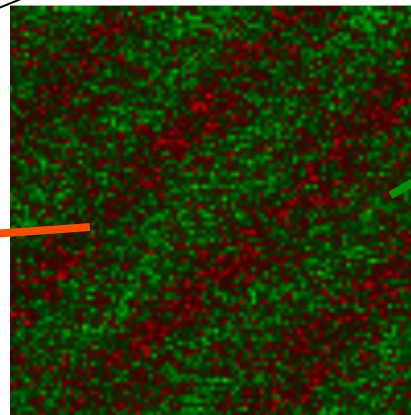
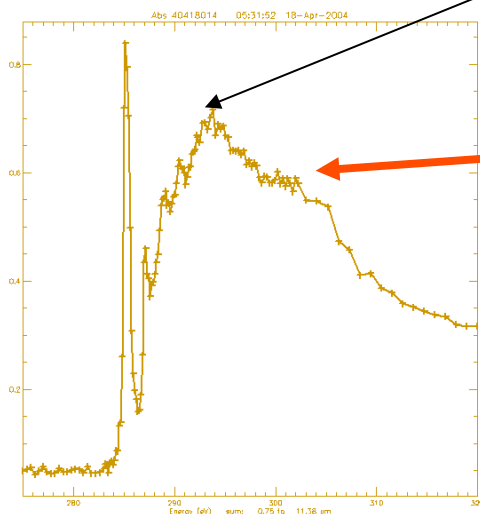
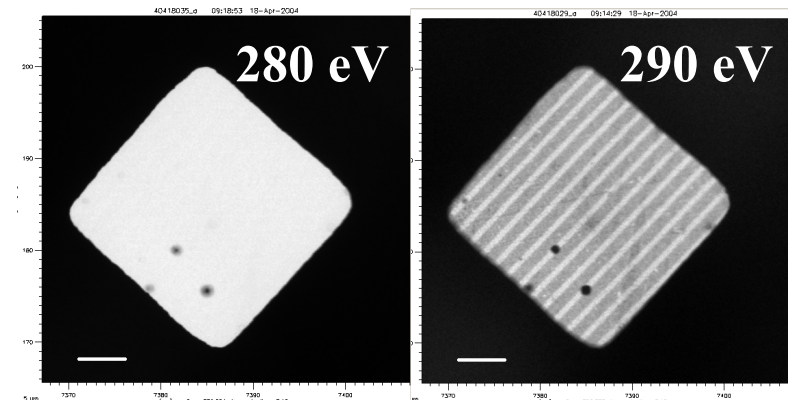
Sample from: John Lawrence, George Swerhone (NWRI-Saskatoon), Gary Leppard (NWRI-CCIW)

# A. Hitchcock, McMaster U.



M.K. Gilles, R. Planques, S.R. Leone  
LBNL  
Samples from B. Hinsberg, F. Huele  
IBM Almaden

Exposure to UV light results in loss of carbonyl peak



Map chemical spectra taken of pure samples  
onto a sample containing both components

Courtesy of Mary Gilles, LBNL



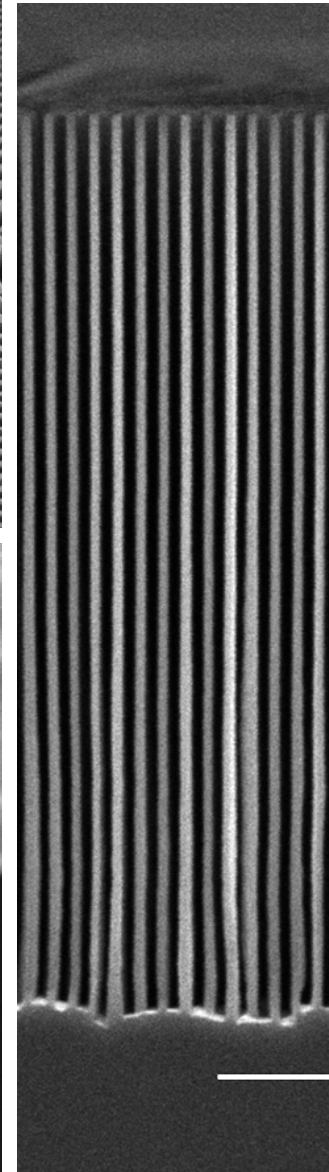
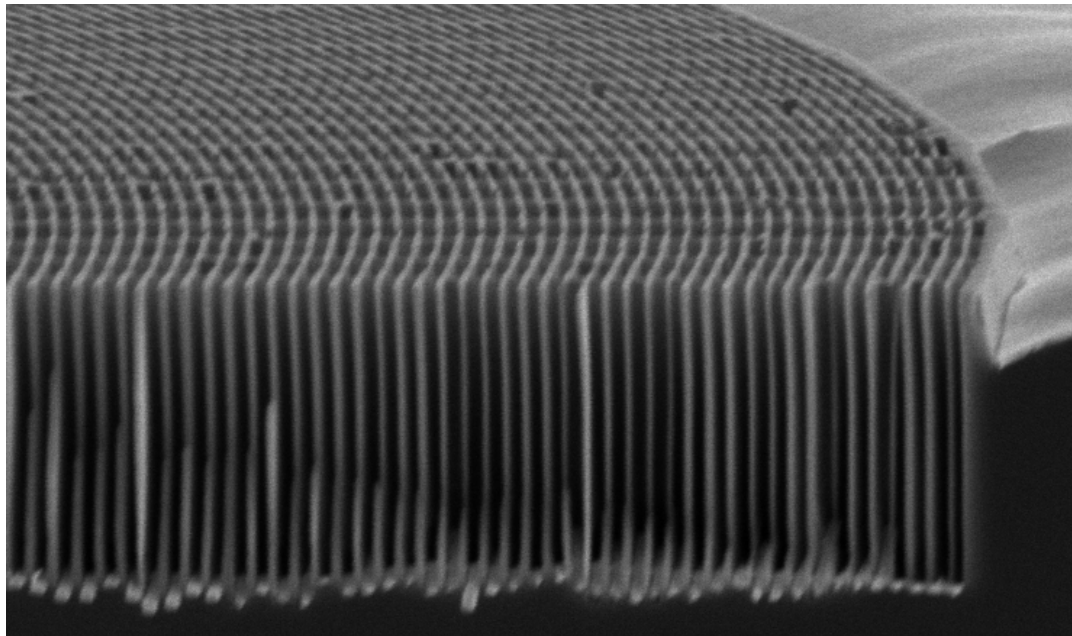
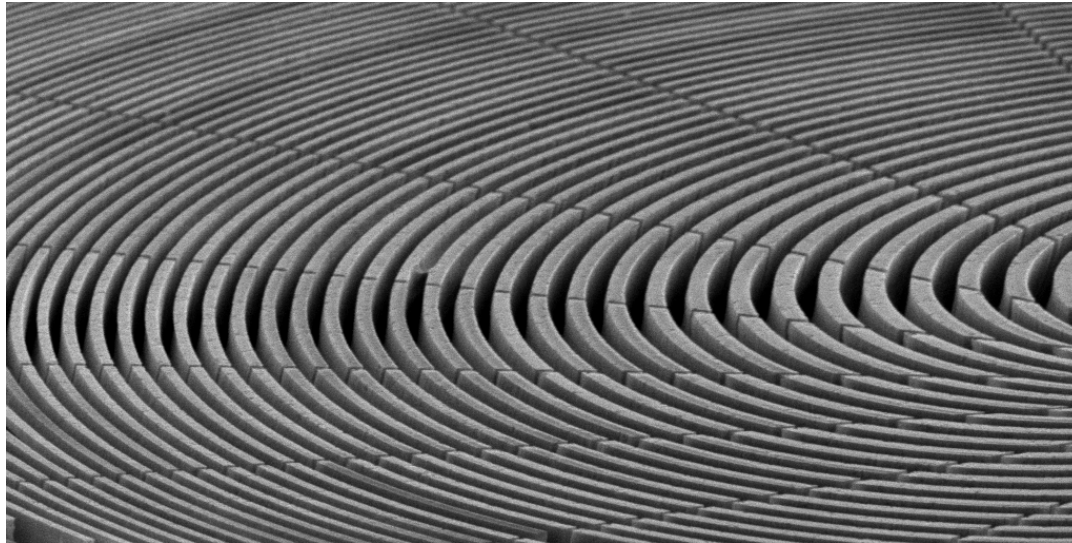
# Hard x-ray zone plate microscopy

---

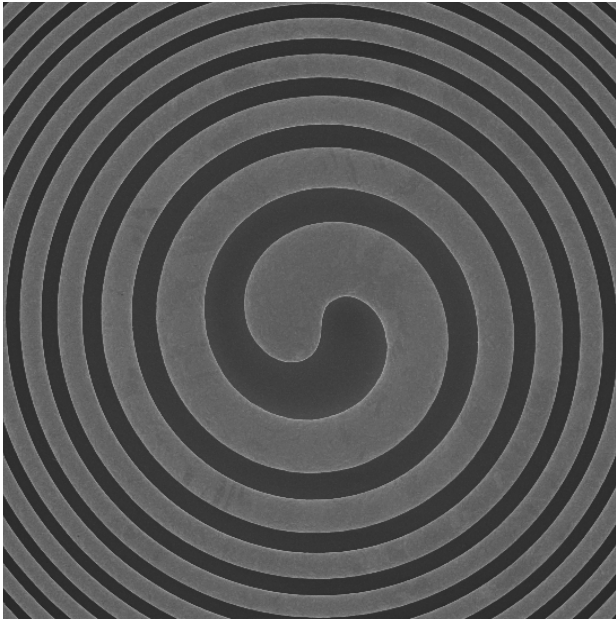


- Shorter wavelengths, potentially better spatial resolution and greater depth-of-field.
- Less absorption ( $\beta$ ); phase shift ( $\delta$ ) dominates, higher efficiency.
- Thicker structures required (e.g., zones), higher aspect ratios pose nanofabrication challenges.
- Contrast of nanoscale samples minimal; will require good statistics, uniform background, dose mitigation.

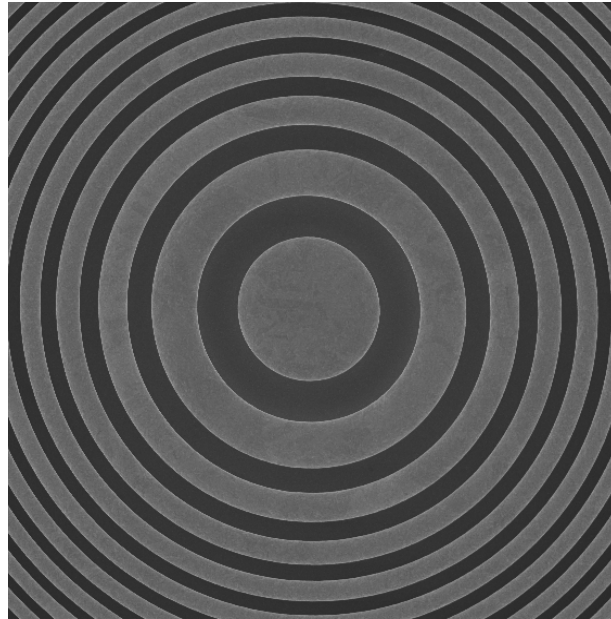
# Ultra high aspect ratio nanofabrication of high efficiency, high resolution x-ray zone plates for the 50 eV-30 keV regime



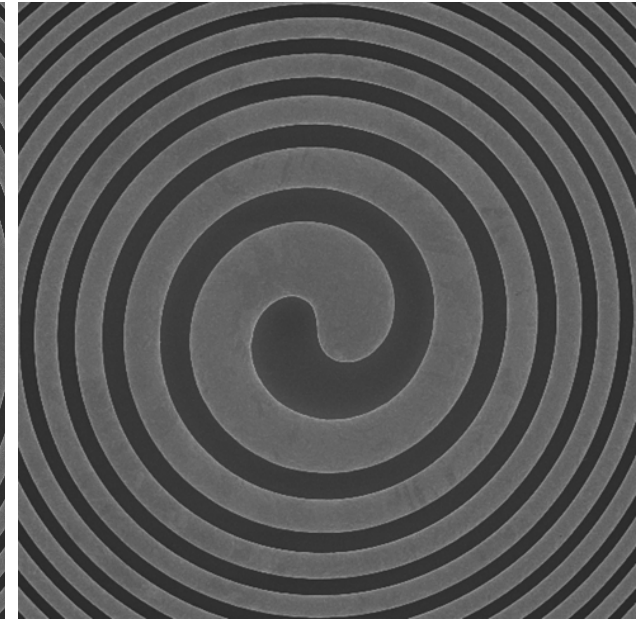
# X-ray focusing with orbital angular momentum control



+1 OAM



No OAM

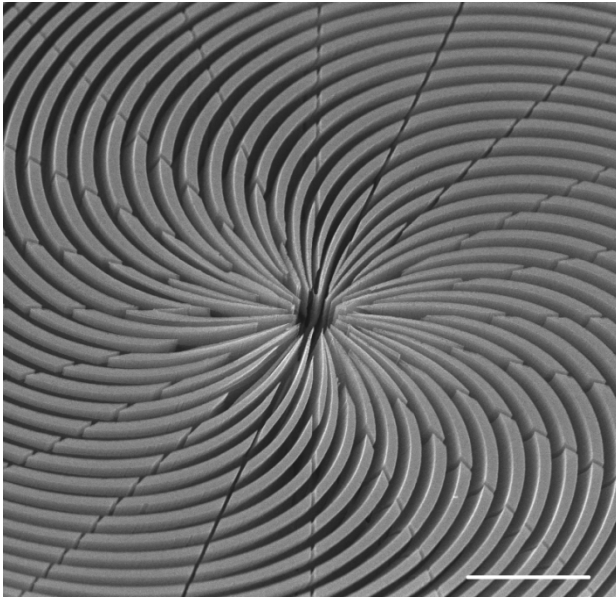


-1 OAM

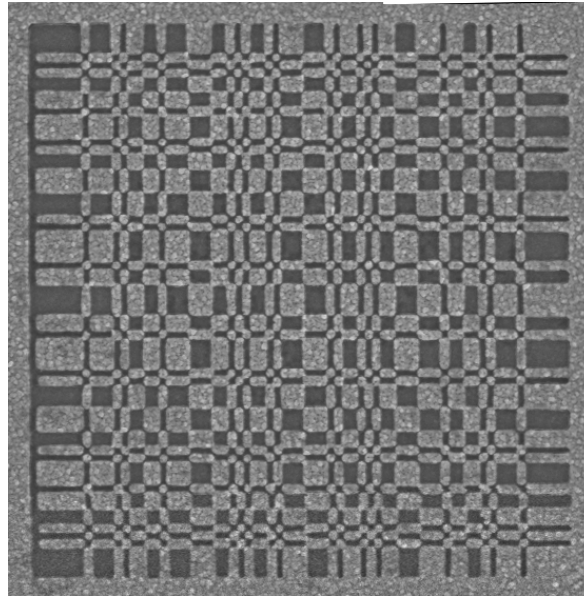
X-rays with various amounts of orbital angular momentum can be produced using a spiral zone plate structure. These spiral zone plate structures can also be used in place of the objective zone plate in an x-ray microscope for phase contrast imaging.



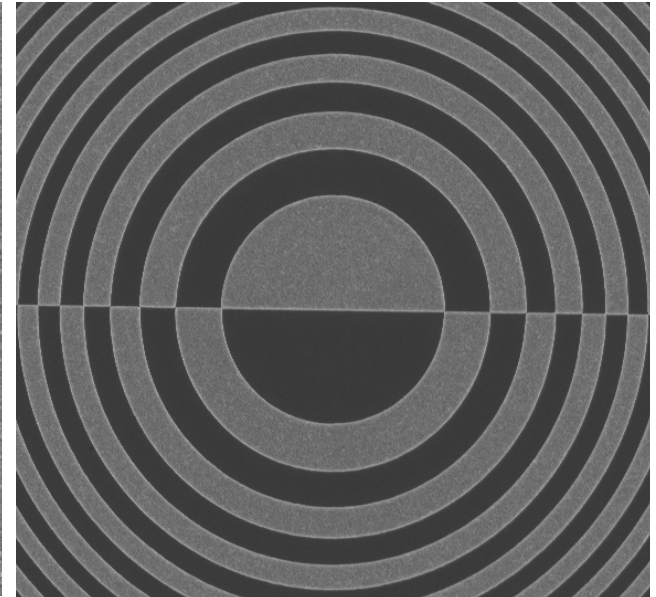
# Specialized x-ray diffractive optical elements enable new science at synchrotron facilities



Spiral zone plate for producing x-rays with charge 50 orbital angular momentum



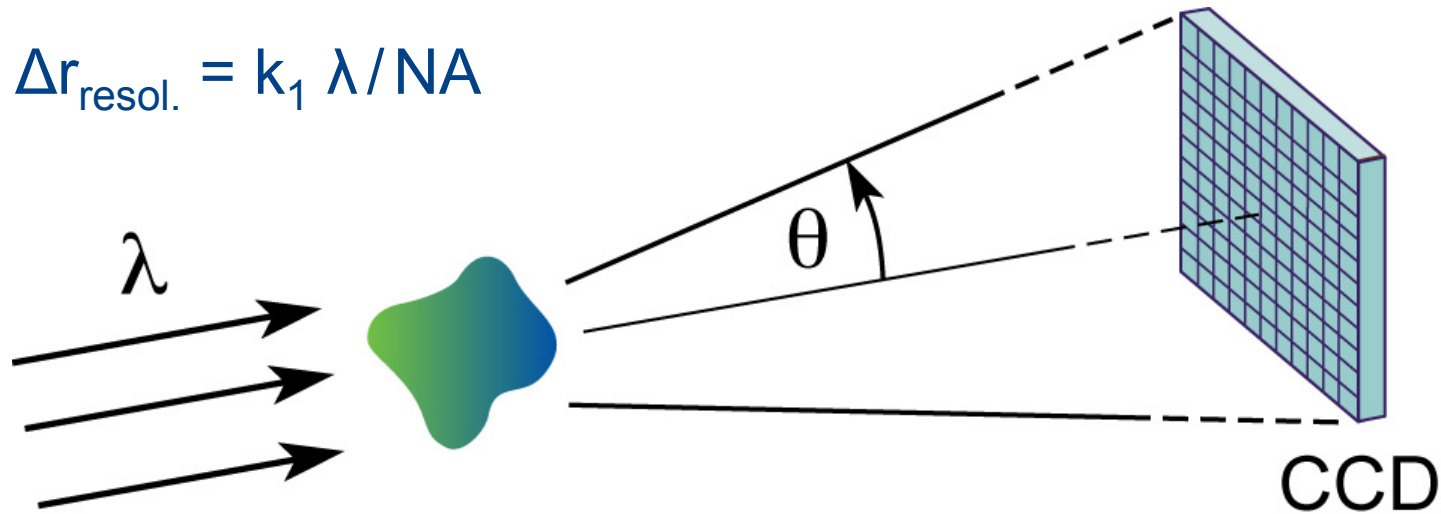
Uniformly redundant array for x-ray parallel holography, alignment, and other applications



Zone plate for x-ray differential interference contrast microscopy

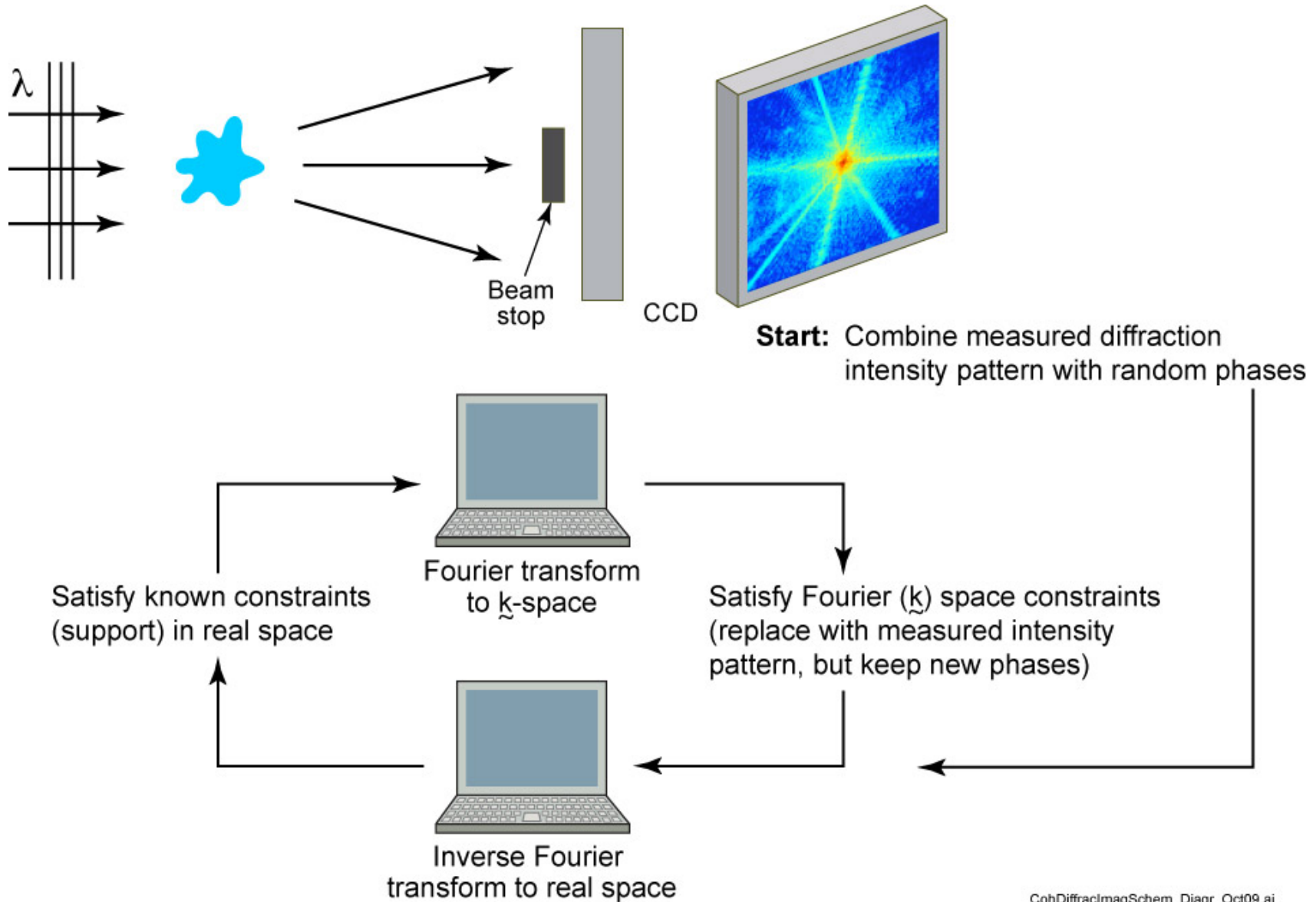
## A lens is not necessarily required

$$\Delta r_{\text{resol.}} = k_1 \lambda / \text{NA}$$

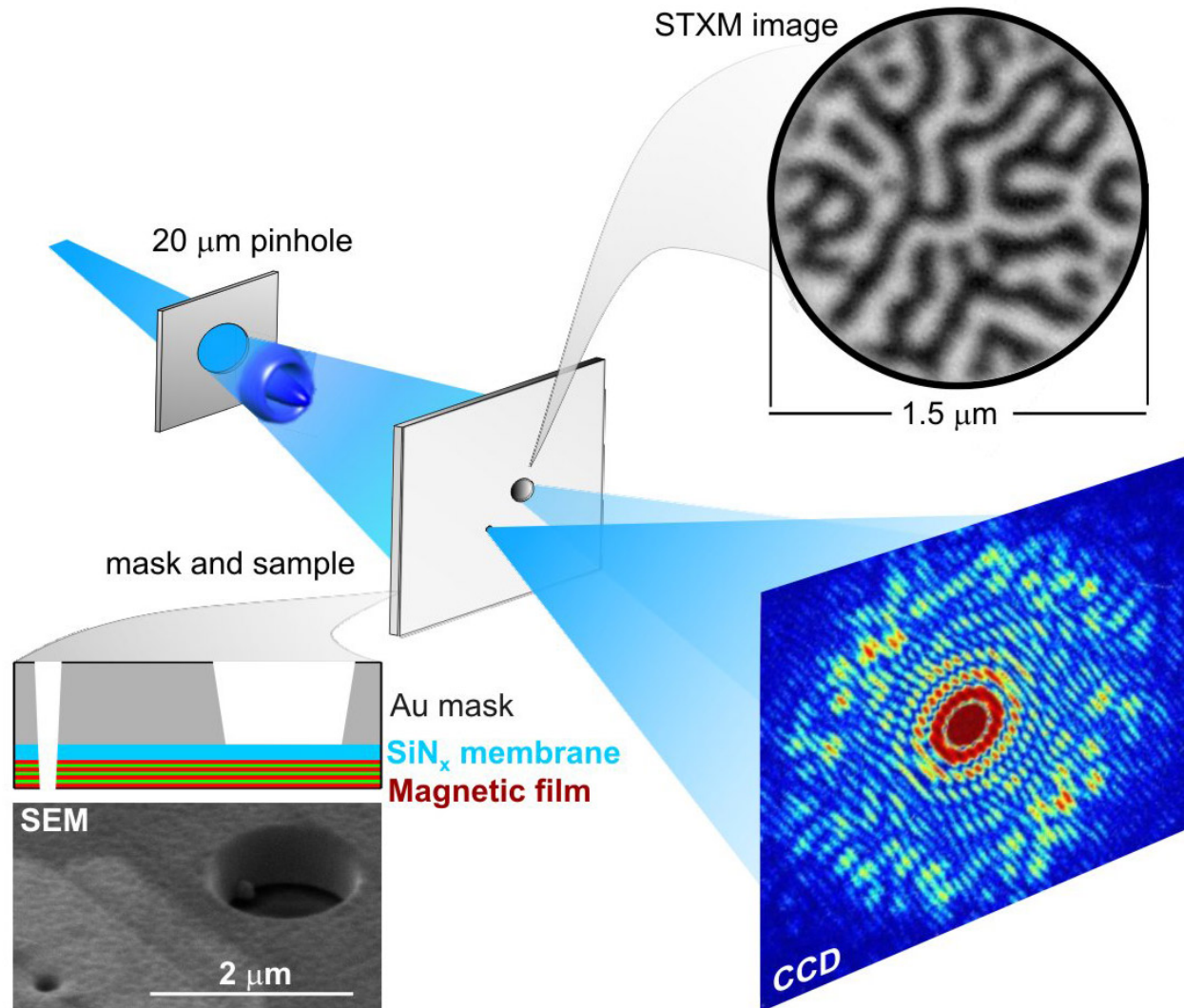


“Lensless” coherent diffraction imaging (CDI) is being aggressively pursued.

# Coherent diffractive imaging (CDI)



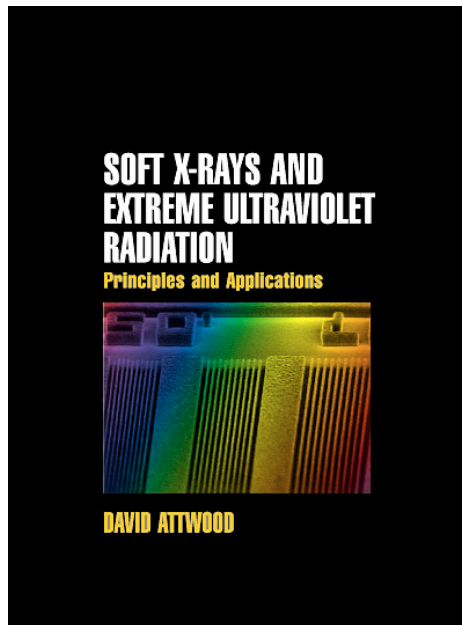




S. Eisebitt, J. Lüning, W.F. Schlotter, M. Lörger, O. Hellwig,  
W. Eberhardt & J. Stöhr / *Nature*, 16 Dec 2004

LenslessImagingF1.ai

# Lectures online at [www.youtube.com](http://www.youtube.com)



Amazon.com



**UC Berkeley**

[www.coe.berkeley.edu/AST/sxreu](http://www.coe.berkeley.edu/AST/sxreu)

[www.coe.berkeley.edu/AST/srms](http://www.coe.berkeley.edu/AST/srms)

[www.coe.berkeley.edu/AST/sxr2009](http://www.coe.berkeley.edu/AST/sxr2009)